Journal Pre-proof

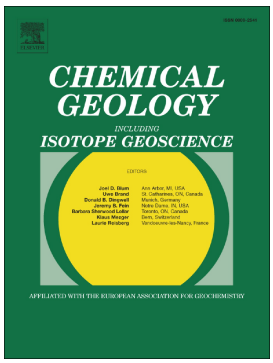

Inheritance versus subduction-related δ11B signatures of eclogites: Insights from the Voltri Massif (Ligurian Western Alps, Italy)

Enrico Cannaò, Marco Scambelluri, Othmar Müntener, Benita Putlitz, Samuele Agostini

PII: S0009-2541(22)00512-5

DOI: https://doi.org/10.1016/j.chemgeo.2022.121218

Reference: CHEMGE 121218

To appear in: *Chemical Geology*

Received date: 28 July 2022

Revised date: 4 November 2022

Accepted date: 13 November 2022

Please cite this article as: E. Cannaò, M. Scambelluri, O. Müntener, et al., Inheritance versus subduction-related δ11B signatures of eclogites: Insights from the Voltri Massif (Ligurian Western Alps, Italy), *Chemical Geology* (2022), https://doi.org/10.1016/j.chemgeo.2022.121218

Inheritance *versus* subduction-related $\delta^{11}B$ signatures of eclogites: insights from the Voltri Massif (Ligurian Western Alps, Italy)

Enrico Cannaò[1,*], Marco Scambelluri[2], Othmar Müntener[3], Benita Putlitz[3] and Samuele Agostini[4]

[1]*Dipartimento di Scienze della Terra "A. Desio", Università degli Studi di Milano, Via S. Botticelli 23, 20133 Milano, Italy*

[2]*Dipartimento di Scienze della Terra, Ambiente e Vita, Università degli Studi di Genova, C.so Europa 36, 16132 Genova, Italy*

[3]*Institute of Earth Sciences, University of Lausanne, 1015 Lausanne, Switzerland*

[4]*Istituto Geoscienze e Georisorse, CNR, Via G. Moruzzi 1, 56124 Pisa, Italy*

[*]*Corresponding author: enrico.cannao@unimi.it*

to be submitted to *Chemical Geology*

Abstract

Trace element and isotopic compositions of exhumed high-pressure (*P*) mafic rocks are an important archive to investigate chemical processes in subduction zones. Here we report the B isotope ($\delta^{11}B$) composition of eclogitic mafic rocks enclosed in high-*P* serpentinite from the Voltri Massif, Ligurian Alps (Italy). Combined with bulk $\delta^{18}O$ values, $^{87}Sr/^{86}Sr$ ratios and trace element data, the $\delta^{11}B$ of eclogitic mafic rocks were investigated to test oceanic inheritance *vs.* subduction-related processes and to provide inferences on the timing of B uptake in eclogitic metagabbros.

Petrographic observations along with major and trace element data indicate that the eclogite facies mafic rocks derived from primitive Mg-Al-bearing gabbros (Erro-Tobbio eclogites) and differentiated Fe-Ti-bearing oxide gabbros (Vara eclogites). Metarodingite from Vara shares similar REE pattern to that of the Erro-Tobbio eclogites, suggesting a plagioclase-rich gabbroic protolith. The studied rocks show variable enrichments in fluids-mobile elements (e.g., Cs, Ba, Li, Sr; high Li/Y, B/Nb). Boron concentrations range between 2.3 to 7.6 ppm, with no significant differences among the different samples. Oxygen isotope compositions ($1\sigma \pm 0.1$‰) for the Vara and the Erro-Tobbio eclogites range from +5.4 to +6.4‰ and from +3.1 to +5.3‰, respectively, whereas the $^{87}Sr/^{86}Sr$ ratios range between 0.7036 and 0.7042 for the Vara eclogites and from 0.7030 to 0.7034 for Erro-Tobbio metagabbros. The B isotope compositions for the Vara eclogites range between -3.2 to +0.9‰, which are in striking contrast with the positive $\delta^{11}B$ signatures of the Erro-Tobbio eclogitic metagabbros ranging from +4.3 to + 8.9‰, the highest positive $\delta^{11}B$ signatures observed in eclogitic metagabbros so far. Metarodingite from Vara has a $\delta^{18}O$ of +3.7‰ and $^{87}Sr/^{86}Sr$ of 0.7046 and a $\delta^{11}B$ value of +11.5‰.

We argue that the $\delta^{18}O$ signatures and the $^{87}Sr/^{86}Sr$ ratios of metamafic rocks from the Voltri Unit mainly reflect inherited signatures from the seafloor, whereas subduction-related processes are mainly traced through $\delta^{11}B$ variations. Progressive B isotope fractionation due to dehydration processes during subduction is responsible for the dominantly negative $\delta^{11}B$ signatures of eclogites from the Vara area and elsewhere, whereas the positive $\delta^{11}B$ of the high-*P* metarodingite is

compatible with an inherited oceanic signature, although interaction with fluids released by the surrounding serpentinites at peak conditions cannot be ruled out. We discuss three scenarios to explain the positive $\delta^{11}B$ imprint reported for the Erro-Tobbio eclogites: (i) inheritance of oceanic signatures, (ii) records of B isotope fractionation from an extreme ^{11}B-rich protolith, or (iii) interaction with ^{11}B-rich slab fluids derived from serpentinite hydration at high-*P*. Based on these scenarios, two potential implications of global relevance are presented: (1) the transfer of largely unmodified oceanic signatures up to eclogite facies conditions, and (2) the formation of newly (subduction-related) ^{11}B-rich reservoirs. We propose that the protolith composition of the mafic crust controls the development of hydrous phases at high-*P* thus enabling the preservation of high $\delta^{11}B$ signatures. This mechanism of chemical transfer may generate a ^{11}B-rich reservoir that, together with high-*P* serpentinites, may form positive $\delta^{11}B$ domains in the mantle.

Keywords: Boron isotopes, Boron recycling, Voltri Massif, Eclogites

1. Introduction

In the last decades estimates of the geochemical fluxes of fluid-mobile elements and volatiles in subduction settings have become increasingly more quantitative (Cannaò and Malaspina, 2018; Mallik et al., 2018; Plank and Manning, 2019). The contribution of serpentinized mantle from both slab and wedge derivation is now ascertained by many studies (Scambelluri et al., 2019, and references therein) and strongly controls the budget of volatiles and incompatible elements at depth exceeding 100 km, beyond the stability of antigorite (Scambelluri et al., 2015; Spandler et al., 2014). Despite a significant early release of fluids and elements at shallow depth (Hacker, 2008; Rüpke et al., 2004; Savov et al., 2005), the role of sedimentary rock in providing volatiles and other chemical components to arc volcanoes and contaminants to the deeper mantle is relevant and mainly controlled on the destabilization of phengite, lawsonite and accessory minerals (Cannaò and Malaspina, 2018; Hermann et al., 2013). Hydrothermal alteration processes in the oceanic crust also have a strong

impact in the amounts of volatiles and fluid-mobile elements released at depth in convergent margins (Cannaò and Malaspina, 2018, and references therein); however, the composition of altered oceanic crust (AOC) can be extremely variable depending on the alteration degree of the original protolith (Staudigel, 2014) and its parental composition (Godard et al., 2009). Depending on the whole rock chemistry (e.g., Mg-Al gabbro *vs.* Fe-Ti gabbros), different high-pressure (*P*) mineral assemblages may develop (Angiboust et al., 2012; Pelletier and Müntener, 2006). Early models emphasized that the major fluid pulse from subducted AOC was linked to the destabilization of amphibole during the blueschist-eclogite transition (Peacock, 1993). Experimentally-determined phase equilibria at high-*P* have shown that other hydrous phases such as lawsonite, chloritoid, talc and epidote can be present in mafic systems (Poli, 1995; Poli and Schmidt, 1997, 1995). These phases can release fluids at greater depths; however, how the compositional variability of the AOC affects the release and mobility of fluid-mobile elements in subduction zones is poorly explored (e.g., Spandler et al., 2003). To better understand fluid-mobile element and volatile cycles in convergent margins fluid-rock interactions among different slab lithologies are crucial (Bebout and Penniston-Dorland, 2016). Deciphering between oceanic inheritance *versus* subduction-related signatures in high-*P* rocks is a challenging task requiring both trace element and isotopic data. To this end, the boron (B) isotope systematics ($\delta^{11}B$) has revealed as a powerful tracer of rock dehydration and fluid/rock interaction processes in subduction zones (de Hoog and Savov, 2018; Leeman and Sisson, 1996) and the B isotope studies of subduction-derived rocks are of particular interest to constrain the geochemical evolution of metamorphic terranes (Cannaò et al., 2015; Halama et al., 2020; King et al., 2007; Prigent et al., 2018). The fluid-mobile nature of B coupled to large B isotope fractionation makes B an ideal tracer for fluid processes during progressive rock dehydration (Bebout and Nakamura, 2003; Rosner et al., 2003). The preferential loss of B and of its heavy isotope to fluids results in a B-poor and isotopically light (*i.e.*, ^{11}B-poor) eclogitic residue in subducting slabs (King et al., 2007; Pabst et al., 2012; Peacock and Hervig, 1999). In this contribution, we provide new insights into the $\delta^{11}B$ fingerprints of eclogitized mafic rocks of the Voltri Massif (Ligurian Western Alps, Italy) showing

both negative and positive $\delta^{11}B$ signatures, the latter documented here for the first time. We discuss scenarios where the ^{11}B-enriched signatures of the Voltri rocks can either represent an oceanic inheritance, or an interaction with slab-derived fluids during prograde subduction. Timing of B uptake in these rocks is also discussed in the light of $\delta^{18}O$ values, $^{87}Sr/^{86}Sr$ ratios and trace element data. We speculate that oceanic mafic rocks and the eclogites experiencing fluid-mediated exchange with serpentinites at high-*P* represent ^{11}B-rich reservoirs transferring their positive $\delta^{11}B$ signatures to depth.

2. Geological background

The Voltri Massif consists of ophiolitic rocks associated with metasediments (**Fig. 1**) and recorded initial oceanic alteration followed by eclogite-facies subduction and exhumation during the Alpine orogeny (Crispini and Capponi, 2007). The dominant rock types of the Voltri Massif are metamorphosed antigorite-bearing serpentinites, peridotites and mica-/calc-schists associated with metavolcanics of oceanic origin (Capponi et al., 2016; Chiesa et al., 1975). Smaller (1 – 100 m) metamorphosed gabbroic and basaltic bodies are embedded within ultramafic rocks and metasediments (Malatesta et al., 2012). Metamorphosed rodingite dikes are often enclosed in serpentinites as witness of oceanic alteration on the seafloor (Haws et al., 2021; Scambelluri and Rampone, 1999). According to the recent revision of the tectonic evolution by Capponi et al. (2016), the Voltri Massif consists of three major tectono-metamorphic Units: the Varazze, Palmaro-Caffarella and Voltri Units (**Fig. 1**) showing increase in peak metamorphic conditions from greenschist- to blueschist- to eclogite-facies conditions, respectively. The samples investigated in this work are from the Voltri Unit; however, in this contribution, we treat the samples pertaining to the Erro-Tobbio sliver distinct from the other serpentinites and eclogites of the Voltri Unit, which are reported hereafter as the Vara eclogites, located in the central sector of the massif (**Fig. 1**). The peak metamorphic conditions in the Voltri Unit are recorded by garnet-pyroxene assemblages in mafic rocks, phengite-garnet assemblages in metasediments and of metamorphic olivine, Ti-clinohumite,

magnetite and diopside either in veins and overgrowing antigorite in massive and foliated high-*P* serpentinites (Scambelluri et al., 1995, 1991). Estimated peak metamorphic conditions range between 1.8 and 2.5 GPa and from 450 to 600 °C (Brouwer et al., 2002; Federico et al., 2007; Liou et al., 1998; Malatesta et al., 2012; Scambelluri et al., 2016; Scarsi et al., 2017; Starr et al., 2020; Vignaroli et al., 2005). The ages of the prograde, peak and retrograde assemblages of the Voltri Massif span from 50 to 33 Ma (Federico et al., 2005; Haws et al., 2021; Rubatto and Scambelluri, 2003; Starr et al., 2020; Vignaroli et al., 2010). Recent geochronology using Sm-Nd systematics on garnet constraints the peak age at ~ 40 ± 2 Ma (Starr et al., 2020) for the Vara eclogites. Similarly, high-*P* recrystallization ages of the metarodingite bodies obtained with Sm-Nd systematics on garnet gave 40.6 ± 2.9 Ma, whereas a garnetite vein cross-cutting a main metarodingite body is dated at 37.7 ± 1.4 Ma, near peak eclogites-facies conditions (Haws et al., 2021). Further details about the geological background of the Voltri Massif can be found in the **Supplementary Materials**.

3. Sample description

In this study, we analyzed eclogitic metagabbros and one eclogitic metarodingite from the Vara area (near the Vara village, **Fig. 1**) and several eclogitic metagabbros from the Erro-Tobbio, in the north-eastern sector of the massif (**Fig. 1**). The petrographic and petrologic features of the Vara rocks are well known (Bocchio, 1995; Cimmino et al., 1981; Cortesogno et al., 1977; Haws et al., 2021; Messiga et al., 1983; Messiga and Scambelluri, 1991; Scambelluri and Rampone, 1999; Starr et al., 2020). Detailed petrographic and petrologic descriptions of the Erro-Tobbio eclogites are presented by Messiga et al. (1995); in addition, these rocks have been analyzed for their O-H isotope compositions (Früh-Green et al., 2001), and one eclogite sample (E89-26) was also analyzed for its [B], $\delta^{11}B$ and $^{87}Sr/^{86}Sr$ (Scambelluri and Tonarini, 2012). Here we summarize the key features of the studied samples (**Table 1**), referring to previous works for more exhaustive descriptions.

The Erro-Tobbio metagabbros are associated with mantle peridotites and high-*P* serpentinites (Früh-Green et al., 2001; Scambelluri et al., 2001). Their protoliths were troctolite and (olivine) gabbros

intruded in partially serpentinized mantle rocks and affected by subsequent subduction to eclogite-facies condition during the Alpine orogeny (Messiga et al., 1995). The eclogite facies recrystallization occurs statically, forming corona structures (samples MG5, F1, MG4/7) as well as dynamically, developing mylonitic textures along former stretched magmatic minerals (sample E89-26). Coronitic rocks preserve the original textures of low-*P* cumulates showing idiomorphic olivine, plagioclase and interstitial clinopyroxene (Borghini et al., 2007). With the exception of rare clinopyroxene and rare plagioclase and olivine relicts, igneous minerals were pseudomorphosed by high-*P* mineral assemblages. Igneous plagioclase and olivine were replaced by jadeite + zoisite ± garnet and talc + tremolite, respectively; omphacite + talc developed after magmatic clinopyroxene. Omphacite + talc + garnet coronas developed along the clinopyroxene/plagioclase boundaries (Früh-Green et al., 2001; Messiga et al., 1995) while chloritoid + talc + garnet coronas (*type 2* in Messiga et al., 1995) developed between igneous olivine and plagioclase domains. Locally, orthopyroxene is stable with chlorite and garnet (*type 1* in Messiga et al., 1995) replacing magmatic olivine sites in sample MG4/7 which, in turn, is replaced by *type 2* corona (see Messiga et al., 1995; **Table 1**). In the mylonitic sample E89-26, the stretched magmatic mineral sites are still distinguishable. The rock shows a banded texture consisting of alternating fine-grained layers of omphacite + garnet ± chlorite with omphacite porphyroclasts, omphacite + zoisite ± garnet and omphacite + talc + chloritoid that correspond to pseudomorphs after primary clinopyroxene, plagioclase and olivine domains. To summarize, the association of chlorite + garnet ± chloritoid and chloritoid + talc ± garnet in coronas is coeval with the high-*P* assemblages made of jadeite + zoisite ± garnet and omphacite + garnet in microdomains. This textural relationship likely indicates hydration at high-*P* conditions (Messiga et al., 1995).

In the Vara area, the core of the Voltri Unit (**Fig. 1**), mylonitic olivine-bearing high-*P* serpentinites enclose boudinaged mylonitic Fe-Ti-oxide rich eclogites (samples ENV1, ENV10/2, FL4) and metarodingites (sample ENV11B). In this configuration, the antigorite foliation formed during subduction-zone eclogitization of the associated mafic bodies (Cannaò et al., 2016; Haws et al.,

2021). In thin section, the Vara mylonitic eclogites display porphyroclastic omphacite embedded in a foliated fine grained omphacite matrix hosting zoned almandine-rich garnet and oriented rutile stripes (**Fig. 2A**). Accessory quartz, magnetite and sulfide are also present. Glaucophane can be stable with omphacite and garnet, although it more generally overgrows omphacite (Gln in **Fig. 2A**); late actinolite ± diopside and albite form along the glaucophane rims and in the core of the omphacite porphyroclasts. The above secondary assemblages are compatible with retrograde blueschist- and greenschist-facies conditions. Sample ENV10/2 is representative for a garnet-rich layer within the eclogite bodies (**Fig. 2B**) whereas samples ENV1 and FL4 represent foliated metagabbros with almost equal and comparable amount of garnet and omphacite. Sample FL4 shows higher amounts of retrograde glaucophane.

Metarodingite ENV11B shows a massive texture with garnet + diopside + chlorite equilibrium assemblages. Apatite, magnetite and titanite are present as accessory minerals, as previously reported (Scambelluri and Rampone, 1999). Recrystallization of garnet and diopside (Di2 in **Fig. 2C**) along the grain boundaries and in veins are indicative of high-*P* metamorphic conditions (Haws et al., 2021).

A striking difference between Erro-Tobbio and Voltri eclogites regards the protolith composition: the Vara eclogites derived from Fe-Ti oxide rich metagabbros, as shown by high modal rutile, and the Erro-Tobbio eclogites correspond to Mg-Al gabbros (Messiga et al., 1995). The eclogitic assemblage of the Vara rocks is dominated by anhydrous minerals, while abundant hydrous phases in the Erro-Tobbio high-*P* assemblage points to uptake of significant amount of H_2O in these rocks.

4. Methods

Major and trace element concentrations of metamafic rocks were determined by laser ablation inductively coupled plasma mass spectrometry (LA-ICP-MS) on pressed powder pellets (PPP) at the Geochemistry, Geochronology and Isotope Geology laboratory hosted at the Earth Science Department, University of Milano (Italy). The instrument couples an Analyte Excite 193 nm ArF excimer laser microprobe system equipped with a double volume chamber cell HelEx II (Teledyne

Cetac Technologies) to a single-quadrupole ICP-MS (iCAP-RQ, Thermo Fisher Scientific). Reported final data are the mean of 6 spot analyses and the error is expressed as their standard deviation (1σ). Precise B concentrations were determined by isotope dilution using the NIST SRM 982 as spike and determined using a single collector VG Isomass 54E P-TIMS (now dismissed) running in dynamic mode at the IGG-CNR, Pisa (Italy). Boron was extracted through alkaline fusion and purification by three-step ion-exchange technique and boron isotope composition was determined via Multi-Collector ICP-MS at the IGG-CNR, Pisa (Italy) as described in Agostini et al. (2021). The oxygen isotope composition was determined by using a CO_2-laser fluorination line coupled to a Finnigan MAT 253 mass spectrometer hosted at the Institute of Earth Science, University of Lausanne (Switzerland). Oxygen and B isotope compositions are reported in the standard delta(δ)-notation (expressed in permil ‰), relative to VSMOW and NIST SRM 951 standards, respectively. Strontium isotope analyses were performed via Multi-Collector ICP-MS at the IGG-CNR, Pisa (Italy) as described in Agostini et al. (2022). In order to constrain the influence of the H_2O on the formation of hydrous-bearing assemblages at high-*P* conditions for the Erro-Tobbio eclogites (former oceanic Mg-Al gabbros), *T*-X_{H2O} isobaric (*P* =2.5 GPa) and *P*-X_{H2O} isothermal (*T* = 550 °C) equilibrium phase diagram modeling was carried out through Gibbs free energy minimization using the program Perple_X (Connolly, 2005). The average composition of the olivine-bearing gabbros from IODP site U1309 (Godard et al., 2009), representing the oceanic equivalent of the Erro-Tobbio eclogites, was used for the calculations in the simplified system SiO_2-Al_2O_3-MgO-FeO-CaO-Na_2O with a H_2O content ranging from 0 to 4 wt.%. Further information about the analytical methodology and the thermodynamic modeling can be found in the **Supplementary Materials**.

5. Results

5.1. Major and trace element composition

Major, minor and trace element compositions of the studied metamafic rocks are reported in **Table 2**. The main feature of the Vara eclogites area are their high contents in Fe_2O_3 and TiO_2 (up to 21.3

and 6.1 wt.%, respectively), suggesting derivation from differentiated Fe-Ti gabbros. The Erro-Tobbio eclogites are mostly depleted in these oxides showing strong enrichment in MgO and Al_2O_3 (up to 11.6 and 20.0 wt.%, respectively), typical features of Mg-Al gabbroic bodies intruded into the oceanic lithosphere. Metarodingite shows the alkali-silica depletion (Na_2O and K_2O below 0.1 wt.%) and CaO enrichment (25.5 wt.%) characteristic of rodingite processes and metasomatism occurring at the seafloor during oceanic low-grade metamorphism (e.g., Bach and Klein, 2009)

The Rare Earth Element (REE) patterns of the eclogites are very different between the Vara and the Erro-Tobbio rocks (**Fig. 3**). The Vara samples ENV1 and FL4 are characterized by slight enrichment and depletion in light-REE (LREE; La_N/Sm_N of 1.12 and 0.70, respectively, and both show slight depletion from middle(M-) to heavy-REE (HREE; $Sm_N/Lu_N \sim 1.22$). Normalized REE are always above the reference N-MORB values (Sun and McDonough, 1989) in agreement with evolved tholeiitic melt with MORB affinity and overlap oxide-gabbros from present-day oceanic lithosphere (e.g., Godard et al., 2009). The eclogite ENV10/2 shows a low La_N/Lu_N ratio of 0.14, in agreement with its garnet-rich nature (**Figs. 2B, 3A**). The Erro-Tobbio eclogites show very similar REE patterns (**Fig. 3B**), characterized by variable trends from LREE to MREE (La_N/Nd_N from 0.69 to 1.44), enrichments in MREE over HREE (Sm_N/Lu_N from 1.24 to 1.47) and a striking positive Eu anomaly (Eu_N/Eu_N^* from 1.49 to 3.29) reflecting plagioclase accumulation in the gabbroic protolith. These REE patterns resemble those of preserved troctolites and olivine-gabbros of the Erro-Tobbio rock suite (Borghini et al., 2007) and of drilled slow-spreading oceanic gabbro (e.g., Godard et al., 2009) and related to differentiated cumulus rocks produced by fractional crystallization of a rather primitive N-MORB-type aggregated basalt (Borghini et al., 2007). Metarodingite from Vara share similar REE pattern to that of the Erro-Tobbio eclogites ($La_N/Nd_N = 0.92$; $Sm_N/Lu_N = 1.28$; $Eu_N/Eu^*_N = 2.26$), although showing slightly enriched values relative to N-MORB (**Fig. 3A**).

Normalized to N-MORB (Sun and McDonough, 1989; Marschall et al., 2017), the trace element patterns for the Vara eclogites are heterogeneous (**Fig. 3C**), with sample ENV10/2 showing depletion in all elements except for Cs, B and Sb. Comparable enrichments in these elements are shown by

samples ENV1 and FL4 although the remaining elements are slightly higher than N-MORB values. Metarodingite shows the same depletion in LILEs as for eclogites except for Cs and other fluid mobile elements such as B, Sb and Li (**Fig. 3C**). The trace element patterns for the Erro-Tobbio eclogites show variable enrichments in incompatible elements such as Cs, Ba, B, Sb, Sr and Li and depletion in high field strength elements (Nb, Ta, Zr, Hf), Th, U and Y relative to N-MORB (**Fig. 3D**). Overall, B concentrations range between 2.3 and 7.6 ppm, with no significant difference between Vara and Erro-Tobbio eclogites. Boron contents are not affected by differences in composition and textures of the samples (coronitic *vs.* deformed varieties), although the Erro-Tobbio rocks show slightly more scattered values (**Figs. 3C, D and 4A, C**).

Fluid-mobile (Sr, Ba, Li, B) *versus* fluid-immobile (Nd, Nb, Zr, Y) elemental ratios (**Fig. 5**) for the Erro-Tobbio eclogites show positive trends in Zr/Nb *vs* Sr/Nd, Ba/Nb Li/Y and B/Nb (**Figs. 5A-D**), in Li/Y *vs* Sr/Nd, Ba/Nb and B/Nb (**Figs. 5E-G**) and in B/Nb *vs* Sr/Nd (**Fig. 5H**) diagrams. This demonstrates the fluid-mobile enriched nature of the Erro-Tobbio eclogites compared to precursor troctolite and olivine-gabbro from Erro-Tobbio and from slow-spreading oceanic lithosphere (Godard et al., 2009). The Fe-Ti eclogites from Vara plot mostly within the field of oceanic oxide gabbros (e.g., Godard et al., 2009), with elemental ratios close to the N-MORB source (Sun and McDonough, 1989; Marschall et al., 2017) except for the higher B/Nb ratio (**Figs. 5D, G, H**). Metarodingite from Vara are similar to the Erro-Tobbio eclogites (**Figs. 5 C, D, F, G**).

5.2 Stable (B-O) and radiogenic (Sr) isotopic signatures

The stable B-O and Sr isotopic compositions of the studied Voltri metamafic rocks are reported in **Table 3**. Despite similar B contents, the $\delta^{11}B$ signatures of the studied eclogites are highly variable: the Vara eclogites are characterized by values ranging from -3.2 to +0.9‰, in contrast with the signatures of the Erro-Tobbio eclogites showing higher $\delta^{11}B$ values from +4.3 to +8.9‰. The metarodingite has a $\delta^{11}B$ of +11.6‰, significantly higher than the Vara eclogites (**Fig. 4A**).

The Vara eclogites have both mantle-like and slightly ^{18}O-enriched compositions ranging between +5.4 and +6.4‰, whereas the metarodingite has lower $\delta^{18}O$ value of +3.7‰. The $\delta^{18}O$ composition of the Erro-Tobbio eclogites (data from Früh-Green et al., 2001) are depleted and variably ranging from +3.1 to +5.3‰ (mean value of +4.4 ± 0.9‰; **Figs. 4B, C**).

The age-corrected (40 Ma, Starr et al., 2020) $^{87}Sr/^{86}Sr$ ratios for the Vara eclogites range between 0.70363 and 0.70415, whereas the metarodingite shows a slightly higher value up to 0.70447 (37 Ma, Haws et al., 2021). Assuming coeval peak metamorphic age between Vara and Erro-Tobbio rocks, the eclogitic metagabbros of the Erro-Tobbio show more restricted Sr isotopic ratios ranging between 0.70302 and 0.70347, slightly lower compared to the eclogites from the Vara area. Note that due to the high Sr/Rb ratios of the Erro-Tobbio eclogites, the uncertainty in their eclogite-facies ages has a negligible effect on the final $^{87}Sr/^{86}Sr$ ratios and their interpretation (see **Table 3**). Overall, reported $^{87}Sr/^{86}Sr$ ratios for Vara and Erro-Tobbio eclogites overlap those of non-subducted gabbros from the N. Apennine (Italy – from 0.70295 to 0.70457; Schwarzenbach et al., 2021).

5.3 Hydrous phase assemblages and water content for subducted Mg-Al gabbros

In light of the high-*P* mineral assemblages of the Erro-Tobbio eclogites made of clinopyroxene, garnet, talc, chloritoid, chlorite and zoisite, the calculated peak *P-T* conditions are 2.35-2.55 GPa and 520-580 °C (**Fig. 6**), in agreement with the previous estimates (Messiga et al., 1995). At these *P-T* conditions, the H_2O content stored in the minerals ranges between 1.1 and 2.3 wt% (**Fig. 6**). The predicted H_2O contents of the system at these *P-T* conditions fall within the range of H_2O contents of Mg-Al gabbros from the Atlantis Bank (SW Indian Ridge; Kendrick, 2019) and the Atlantis Massif (Mid-Atlantic Ridge; Godard et al., 2009; see **Supplementary Materials**). At fixed *P* of 2.5 GPa free fluid phase can be present at *T* above 600 °C in these range of H_2O contents (**Fig. 6B**) linked to the partial destabilization of hydrous phases (i.e., chlorite and zoisite).

6. Discussion

The stable O, H and B isotopes are sensitive to changes in the chemical-physical conditions of a system (*e.g.*, *T*, pH) and are geochemical tracers of fluid/rock interactions monitoring open *vs.* closed system evolution in high-*P* metamorphic rocks (e.g., Alt et al., 2012; Cannaò et al., 2016; Früh-Green et al., 2001; Lafay et al., 2019; Putlitz et al., 2000). During the oceanic hydration of mafic and ultramafic rocks, the shift of $\delta^{18}O$ with respect to unaltered protoliths (with signature ≈ +5.8‰) is dependent to the temperature (*T*) of alteration, resulting in an ^{18}O-enrichment (*i.e.*, $\delta^{18}O > +5.8‰$) or ^{18}O-depletion (*i.e.*, $\delta^{18}O < +5.8‰$) at *T* below and above than ≈ 300°C, respectively (Wenner and Taylor, 1971). Other parameters influencing the $\delta^{18}O$ of rocks are the fluid composition and the mineral assemblages. Similarly, B isotopes may help unraveling the hydration history of rocks exposed at the ocean floor. The correlation between the $\delta^{18}O$ and $\delta^{11}B$ isotopic compositions of altered gabbroic rocks from several ophiolitic terranes (*e.g.*, Troodos and Oman) and of present-day altered oceanic crust (AOC; **Fig. 4B**), shows that higher-*T* samples with $\delta^{18}O < +5.8‰$ display $\delta^{11}B$ between +10 and +18‰, trending towards the seawater value (~ +39.6‰). Samples altered at lower-*T* are characterized by $\delta^{18}O > +5.8‰$ and by $\delta^{11}B$ from +5 to -2‰ (Smith et al., 1995; Yamaoka et al., 2012, 2015). Bulk B contents show a rough positive correlation with $\delta^{18}O$ (**Fig. 4C**) and is in turn linked with the *T* of alteration. This chemical modification allows transferring seawater-derived B and O signatures to the altered oceanic crust, as also indicated by the elevated $^{87}Sr/^{86}Sr$ ratios of the Oman gabbros (Yamaoka et al., 2012) (**Fig. 4D**). These $^{87}Sr/^{86}Sr$ ratios are higher than uncontaminated MORB ($^{87}Sr/^{86}Sr = 0.7025$; Rehkamper and Hofmann, 1997) and are shifted towards Cretaceous seawater of ~ 0.7074 (Mcarthur et al., 2001). These isotope geochemical features represent the main drivers to interpret the data presented here and have to be accounted for subduction-related processes, which can further modify the geochemistry of metamafic rocks, *e.g.*, via stable isotope fractionation (e.g., Früh-Green et al., 2001; Rosner et al., 2003) and fluid-mediated interaction with internal or external sources (Barnes et al., 2014; Cannaò et al., 2016, 2015; Scambelluri and Tonarini, 2012).

6.1 Oceanic inheritance vs. subduction-related evolution

6.1.1 Vara eclogites (ENV1, ENV10/2, FL4)

The dominantly negative $\delta^{11}B$ trend of the Vara Fe-Ti oxide rich eclogites contrasts with the common $\delta^{11}B$ fingerprints of the AOC from modern and fossil settings (*e.g.*, obducted Oman and Troodos), showing $\delta^{11}B$ values ranging from 0 to +25‰ and only a few samples with negative $\delta^{11}B$ down to -2‰ (**Fig. 4A**). According to several studies (Smith et al., 1995; Yamaoka et al., 2012), the average [B] and $\delta^{11}B$ signature of the AOC entering in subduction is about 3.6-5.2 ppm and +3.7 to +7.9‰, respectively. Therefore, the low $\delta^{11}B$ signatures shown by the Vara eclogites cannot be explained by oceanic inheritance only, but rather reflect subduction-related processes. It is known from literatures that progressive slab devolatilization during subduction shifts the $\delta^{11}B$ signature of the subducting rocks towards more ^{11}B-depleted values (Rosner et al., 2003). In subduction zones, the B isotope fractionation is mainly driven by the *T* variations within and atop the subducting slab and is more pronounced at low-*T* (Rosner et al., 2003) – *i.e.*, at shallow subduction depths. The $\delta^{11}B$ compositions of the Vara eclogites closely overlap the ones of mafic blueschist-facies minerals recovered from the active subduction zone in the Mariana trench (Pabst et al., 2012) and of high-*P* mafic rocks from fossil subduction zones (King et al., 2007; Martin et al., 2016; Peacock and Hervig, 1999) (**Fig. 7**). This indicates that the Vara eclogites record B isotope fractionation during subduction-zone dehydration and eclogite facies recrystallization. This is confirmed by the anhydrous nature of their peak mineralogy, made of omphacite + garnet + rutile. The slightly positive $\delta^{11}B$ value of ca. +0.9‰ shown by sample FL4 may be related to a partial contribution of retrograde glaucophane due to re-hydration event(s) during initial stage(s) of exhumation. Although the B isotope compositions of the Vara Fe-Ti eclogites can be attributed to prograde metamorphism, their $\delta^{18}O$ composition averaging at +5.8 ± 0.5‰ appears to reflect the initial oceanic imprint (Barnicoat and Cartwright, 1997; Cartwright and Barnicoat, 1999; Putlitz et al., 2000) (**Figs. 4B, C**). Similarly, the $^{87}Sr/^{86}Sr$ ratios of the Vara eclogites reflect the oceanic imprint: their values between 0.70365 and 0.70418 well match those of the non-subducted oceanic crust of Cretaceous age (Yamaoka et al., 2012) and the $^{87}Sr/^{86}Sr$

ratio variability shown by the non-subducted gabbros of the N. Apennine (from 0.70295 to 0.70457; Schwarzenbach et al., 2021; **Fig. 4D**). This indicates that the $\delta^{11}B$ is the main isotope marker of the dehydration processes affecting gabbroic rocks during subduction, fingerprinting prograde dehydration and the ability to re-equilibrate at high-*P* with respect to O isotopes. The inherited $\delta^{18}O$ and $^{87}Sr/^{86}Sr$ ratios from the oceanic stage suggest that the dehydration process likely occurred at closed system conditions.

6.1.2 Vara metarodingite (ENV11B)

Differently from eclogites, the $\delta^{11}B$ of +11.6‰ of theVara metarodingite does not appears to record a negative shift induced by dehydration processes during subduction. Same as $\delta^{11}B$, the +3.7‰ $\delta^{18}O$ composition of this metarodingite is different to those reported for the associated eclogites (+5.8 ± 0.5‰; **Figs. 4B, C**), suggesting that oceanic rodingitization took place at high-*T* conditions. This is consistent with the $^{87}Sr/^{86}Sr$ ratio of the metarodingite, which is more radiogenic compared to those of the eclogites (0.70450 *vs.* 0.70365-0.70418), trending towards the value of Jurassic seawater (~ 0.7070, McArthur et al., 2001). To the best of our knowledge, no data of the $\delta^{11}B$ composition of oceanic rodingites are reported in the literature, making thus difficult to constrain the influence of subduction event(s) super-imposed on oceanic hydration. Remarkably, the $\delta^{11}B$ of the Vara metarodingite overlaps the data of the B isotope composition of non-subducted altered oceanic crust *s.l.* (**Fig. 4**). All these geochemical features agree with the high fluid/rock ratio characteristic of the oceanic rodingitization process of the mafic protolith. Interestingly, the metarodingite also shows relatively high Li/Y and B/Nb ratios compared to those of the Vara eclogites (**Fig. 5G**) associated with no significant variation in their Zr/Nb ratios (**Figs. 5C, D**), thus supporting the interpretation of fluid-rock interaction during the alteration process(es).

The petrologic and geochemical evolution of the Voltri and other alpine rodingites during subduction is described in several works (Evans et al., 1979; Haws et al., 2021; Scambelluri and Rampone, 1999; Zanoni et al., 2016). Particularly, Haws et al. (2021) have recently shown that metarodingites from

the Vara area evolved at open system conditions during interaction with serpentinite-derived fluids close to peak eclogite-facies conditions. This is documented by the enrichments in Cr, Ni and Cu and several fluid-mobile elements (FMEs: Li, Rb, Ca and Ba) in diopside + garnet veins cutting a metarodingite comparable to sample ENV11B (**Fig. 2C**). The enrichments in transition metals and FMEs are interpreted to be related to interaction with high-*P* fluids derived from the surrounding antigorite-bearing serpentinites (Haws et al., 2021) that experienced interaction with sedimentary-derived fluids during prograde metamorphism (Cannaò et al., 2016). An intriguing scenario is that the positive $\delta^{11}B$ data reported for the metarodingite also represents the result of the interaction with fluids sourced from the surrounding serpentinites, which is the primary ^{11}B-rich reservoir in subduction zones (de Hoog and Savov, 2018). The occurrence of high-*P* veins made of metamorphic olivine ± Ti-clinohumite witnesses the residue of fluids pathways released from the partial dewatering of serpentinites at increasing *P-T* conditions (Plümper et al., 2017; Scambelluri et al., 1995), fluids that are expected to be ^{11}B-rich as reported previously (Cannaò, 2020; Clarke et al., 2020; Halama et al., 2020; Scambelluri and Tonarini, 2012; Tonarini et al., 2011). The infiltration of such fluids in rodingites at eclogitic conditions (Haws et al., 2021) may shift their $\delta^{11}B$ towards higher values. For this reason, we cannot completely exclude that the positive $\delta^{11}B$ signature reported here for the Vara metarodingite may also derive from partial re-equilibration with metamorphic fluids. Remarkably, fluid-mediated chemical exchanges between rodingitized mafic bodies enclosed in serpentinites during prograde subduction are reported in several localities (e.g., Laborda-López et al., 2020, 2018), however, the behavior of B and its isotopes in such rocks has not been investigated yet. Overall, the paucity of B isotopic signatures of oceanic rodingites and their metamorphosed counterparts strongly hampers our understanding of the B isotopic evolution in such rocks in subduction environments. Although the metarodingite data reported here might be reasonably explained as an oceanic inheritance, reworking of these rocks by subduction processes cannot be completely ruled out. Further geochemical investigations with more representative metarodingites are required to better constrain this scenario.

6.1.3 Erro-Tobbio eclogites (MG5, F1, MG4/7, E89-26)

The positive B isotope values of the Erro-Tobbio Mg-Al-rich eclogites average at +6.5 ± 2.0‰, significantly higher than those measured in other blueschist- and eclogites-facies mafic rocks (Pabst et al., 2012; Peacock and Hervig, 1999) and are uncommon for subducted metagabbros (**Fig. 7**). Again, these positive $\delta^{11}B$ signatures may develop from: (1) an oceanic inheritance, and/or (2) fluid/rock interaction during subduction.

Regarding the first hypothesis, the Erro-Tobbio eclogites can preserve pre-subduction B, O and Sr isotope signatures (**Fig. 4**). According to Früh-Green et al. (2001), the whole-rock $\delta^{18}O$ signatures of the Erro-Tobbio eclogites are ^{18}O-depleted, suggesting high-T (> 300°C) seafloor alteration. Such a seafloor inherited geochemical signature is supported by the similarity in the $\delta^{18}O$ of igneous clinopyroxene relicts with its metamorphic omphacitic counterpart ($\delta^{18}O$ from +4.4 to +5.6‰), thus indicating the preservation of oceanic compositions and the limited isotopic exchange during eclogitization (Früh-Green et al., 2001). Moreover, the $^{87}Sr/^{86}Sr$ composition of Erro-Tobbio eclogites fall below the range of the obducted Oman and N. Apennines gabbros (**Fig. 4D**) and of the Vara eclogites and is close to the depleted MORB mantle (0.7025; Rehkamper and Hofmann, 1997). The above geochemical features point to limited O and Sr isotopic exchange during subduction and to a preservation of the seafloor signatures. Based on these data, we may also interpret the $\delta^{11}B$ of the Erro-Tobbio eclogites as mainly be inherited from the oceanic stage and, for the best of our knowledge, this represents the first report of eclogites with positive B isotope signatures worldwide. Together with high $\delta^{11}B$ imprint, these eclogites are remarkably enriched in B/Nb, Li/Y, Sr/Nd and Ba/Nb ratios (**Figs. 5D, 7**), which positively correlate with the Eu_N/Eu^*_N ratio (**Fig. 8**). The trends reported in **Figure 8** show the strong relationship between the hydration of igneous plagioclase and the B-Li enrichment driven by fluid/rock interaction. The stability of hydrous phases during prograde subduction up to eclogite facies conditions (Poli and Schmidt, 1995, 1997) and the element re-

distribution between minerals at the sample scale during metamorphic reactions (e.g., Spandler et al., 2003) may control the degree of inheritance of their oceanic geochemical imprint (**Fig. 9A**).

Although the B, O and Sr isotope signature of the Erro-Tobbio eclogites can be reasonably attributed to oceanic inheritance, the $\delta^{11}B$ modification towards less positive values during prograde subduction needs further consideration. Two scenarios can be considered: (i) the occurrence of B isotope fractionation starting form extremely high $\delta^{11}B$ protoliths (**Fig. 9B**), and (ii) the modification of $\delta^{11}B$ values caused by circulating ^{11}B-rich fluids during subduction processes (**Fig. 9C**). In the first case, the B isotope composition of the AOC at 2.4 GPa and 560°C is expected to be ~14‰ lower than that of the oceanic protolith, as modelled by Rosner et al. (2003). Considering the variability of the $\delta^{11}B$ values reported here for the Erro-Tobbio eclogites (from +4 to +9‰), the B isotope composition of the gabbroic protoliths may have ranged between +18 to +23‰. Although the current estimates of the $\delta^{11}B$ signature of the AOC entering in subduction zones comprises between +3.7 and +7.9‰ (Smith et al., 1995; Yamaoka et al., 2012), more recently, a mean $\delta^{11}B$ value of +21.7 ± 1.9‰ has been determined for altered oceanic gabbros (McCaig et al., 2018), thus shifting the upper limit of B isotope signatures of the AOC to much higher values. The calculated B isotope values for the Erro-Tobbio gabbro protoliths agree with the estimation of the $\delta^{11}B$ of present-day altered lower crustal gabbros of the Hess Deep (McCaig et al., 2018), thus supporting the proposed scenario (**Fig. 9B**). However, despite this B isotopic match, the presence of hydrous minerals in the Erro-Tobbio eclogites (Messiga et al., 1995) and their elevated water contents (from 2.6 to 4.4 wt.% of loss of ignition; **Table 2**) suggest that either dewatering of these rocks during subduction was incomplete, or that subduction fluids were added to poorly altered oceanic gabbros, which complicates an evaluation of the $\delta^{11}B$ signatures of their oceanic protolith. Interestingly, the thermodynamic modeling (**Fig. 6**) indicates that the H_2O content required to stabilize the high-*P* mineral assemblage shown by the Erro-Tobbio eclogites is close to the H_2O content of samples F1 and MG 4/7 (**Table 2**), whereas the samples MG5 and E89-26 are characterized by higher H_2O contents (**Table 2**). Remarkably, the latter

samples are the most enriched in Li/Y and B/Nb ratios (**Figs. 5, 8**), indicating higher degree of interaction with fluids.

An alternative interpretation for the positive $\delta^{11}B$ of the Erro-Tobbio eclogites, is an interaction with ^{11}B-rich slab-derived fluids, as proposed by Messiga et al. (1995) to explain the presence of eclogite-facies hydrous minerals in the corona structures separating dry igneous minerals. According to the petrographic and petrologic investigations of the Erro-Tobbio eclogites by Messiga et al. (1995), the development of talc + chloritoid + garnet in corona texture between igneous olivine and plagioclase igneous is indicative of hydration at high-*P* conditions (ca. 2.4 GPa and 550°C, **Fig. 6**). This agrees with the complex history affecting the Erro-Tobbio rock suite as a whole and, in particular, with the geochemical characterization of the enclosing serpentinite, documenting variable interaction with both internally- and externally-derived fluids (Früh-Green et al., 2001; Scambelluri and Tonarini, 2012). The integration of stable O-H and B isotope and Sr isotope systematics highlights that the Erro-Tobbio serpentinite underwent two hydration stages at increasing *T* (*i.e.*, from low grade to high grade serpentinites), as reported by the increase of the H_2O-Sr contents and δD signatures and to the decrease of $\delta^{18}O$ (Früh-Green et al., 2001). Their high B content coupled with their high $\delta^{11}B$ and dissimilar $^{87}Sr/^{86}Sr$ ratios compared to Jurassic seawater, suggest that Erro-Tobbio serpentinites were flushed by Sr- and ^{11}B-rich slab derived fluids during prograde burial and prior to peak conditions (Scambelluri and Tonarini, 2012). As a consequence, the Erro-Tobbio rocks likely evolved along the slab-mantle interface or in supra-subduction environment (Früh-Green et al., 2001; Scambelluri and Tonarini, 2012). The ^{11}B-rich nature of the fluids circulating in such environments is supported by geochemical modelling (*e.g.*, Rosner et al., 2003) and, for instance, the positive $\delta^{11}B$ values shown by tourmaline from eclogitic blocks in the metasomatized mélange overlying the slab from Syros (Greece, Marschall et al., 2006) and forearc serpentinites in the Mariana and South Sandwich trenches (Benton et al., 2001; Tonarini et al., 2011). The relatively high $\delta^{11}B$ values reported for the Erro-Tobbio eclogites therefore could match such a scenario (**Fig. 7**), and they may indicate interaction of the metagabbros with^{11}B-rich slab-derived fluids. The required fluids may derive from the partial

dehydration of the enclosing antigorite-bearing serpentinites linked to the development of olivine-bearing veins during prograde subduction (Messiga et al., 1995; Scambelluri et al., 1995) that, in turn, occurs at open system conditions with external-fluids with an estimated $\delta^{11}B$ of +15‰, as recently proposed by *in-situ* B isotopic data (Clarke et al., 2020). We propose a mechanism involving such ^{11}B-rich hybrid fluids to transfer water and ^{11}B to the Mg-Al eclogites, thus obscuring the B isotope fractionation typical for subducted AOC and, more importantly, mimic the positive $\delta^{11}B$ signatures characteristic of the oceanic alteration stage (**Fig. 9C**). Distinguishing between the proposed scenarios can be accomplished only with further *in-situ* B and O isotopic analyses of the key phases directly involved in the high-*P* evolution of the rocks, mainly chlorite, chloritoid, talc and zoisite (Messiga et al., 1995). These analyses await further development of SIMS or LA-MC-ICP-MS techniques, and further dedicated investigations are necessary to resolve the inheritance *versus* subduction-related $\delta^{11}B$ issue of the Erro-Tobbio eclogites.

6.2 Implications for B cycle

In the previous sections we discussed how the $\delta^{11}B$ signatures of the Voltri eclogites together with others more common geochemical tracers (*e.g.*, O-H, Sr isotope systematics) may help unravelling oceanic inheritance *vs.* subduction-related processes and the open *vs.* closed system evolution of mafic rocks. We have also shown that $\delta^{11}B$ is a powerful isotope tracer of eclogite dehydration processes in the Vara area, having the strongest ability to re-equilibrate relative to other isotope systems. However, the interpretation of the B isotope composition for the Erro-Tobbio eclogites is more controversial and three major scenarios have been proposed (**Fig. 9**): (1) geochemical inheritance of the oceanic stage (**Fig. 9A**), (2) record of the B isotope fractionation from an extremely high $\delta^{11}B$ protolith (**Fig. 9B**), and (3) re-equilibration of the $\delta^{11}B$ imprint by interaction with ^{11}B-rich fluids at high-*P* (**Fig. 9C**). Despite these uncertainties, two potential implications of global importance arise: (i) the transfer of oceanic signatures up to eclogite facies conditions, and (ii) the formation of newly (subduction-related) ^{11}B-rich reservoirs. Based on major and trace element data,

the Erro-Tobbio eclogites derived from primitive Mg-Al-enriched gabbro protoliths while the Vara eclogites have evolved Fe-Ti-oxide gabbro precursors (**Table 2; Fig 3**). We claim that this compositional difference derived from igneous differentiation of tholeiitic basaltic magmas might be the parameter enabling to stabilize hydrous phases in mafic system down to high-*P* conditions, as experimentally reproduced in several works (Schmidt and Poli, 2014, and references therein). Petrology and phase relations of igneous differentiation are responsible for the crystallization of Al-Mg-rich to Fe-Ti-rich gabbros. Based on the geochemistry of present-day slow-spreading oceanic lithosphere from ocean drilling projects (*e.g.*, ODP, IODP), Mg-Al-rich gabbros are generally more abundant than Fe-Ti-rich ones. Mg-Al gabbros can reach 28% of the total volume (vol.%) of the drilled crustal section against the 7 vol.% of the Fe-Ti-rich gabbros in the Atlantis Massif (Mid Atlantic Ridge; IODP Site U1309) (Godard et al., 2009) and up to 78 vol.% of olivine gabbros are reported in the Southwest Indian Ridge (ODP Leg 176 Hole 735B; IODP Hole U1473A) compared with <15 vol.% of Fe-Ti-rich gabbros (Dick et al., 2000; Ferrando et al., 2021). In fast-spreading mid ocean ridges, the volume of Fe-Ti-rich gabbros may increase up to a ratio of 1:1 with Mg-Al gabbros lithology (Wilson et al., 2006), although Fe-Ti-rich gabbros can be virtually absent in the lower oceanic sequence as individuated at the Hess Deep rift Site U1415, East Pacific Rise (Gillis et al., 2014). Consequently, the oceanic alteration of a portion of Mg-Al gabbros can significantly modify their volatile and B budgets and deviate their pristine MORB-like B isotopic signature towards seawater values (*e.g.*, **Fig. 4B**; McCaig et al., 2018). Subduction of such altered gabbros may transfer the oceanic signatures to high-*P* (**Fig. 9A**), as a result of the internal element re-distribution during prograde metamorphic devolatilization reactions facilitated by the stability of hydrous phases in subducted rocks (e.g., Spandler et al., 2003). Based on the total volume of Fe-Ti and Mg-Al gabbros of drilled crustal sections in slow-spreading ridges presented above (Godard et. al., 2009; Ferrando et al., 2020) and considering the average B concentrations of 4.9 and 4.5 ppm for the Vara and Erro-Tobbio eclogites, respectively, we quantify their B flux at high-*P* conditions (**Table 4**). Assuming a convergence rate of 0.05 cm/year and a total arc length of 44000 km (Straub and Layne, 2003), the

maximum B flux contributed by Fe-Ti gabbros and Mg-Al gabbros range between 0.24 to 0.52 x 10^6 mol/year and between 0.84 to 2.33 x 10^6 mol/year, respectively (**Table 4**). Remarkably, the B flux contribution of Mg-Al gabbros is up to 82% (**Table 4**), thus supporting the Mg-Al-rich mafic lithotypes as important ^{11}B-rich reservoir at depth.

The second implication regards the high-*P* hydration of the Mg-Al gabbros as the consequence of dehydration of associated serpentinites, a process releasing ^{11}B-rich aqueous fluids (Cannaò, 2020; Konrad-Schmolke and Halama, 2014; Tonarini et al., 2011). Uprise of these fluids along the slab-mantle interface can be accompanied by interaction with Mg-Al-rich oceanic crust causing its high-*P* hydration with subsequent stabilization of hydrous minerals and storage of ^{11}B (**Fig. 9C**). The mechanism of chemical transfer proposed here has the potential to generate subduction-related ^{11}B-rich reservoirs in the mantle. The quantification of how much B can be transferred with such a mechanism is challenging considering the high variability of slab-mantle interface (e.g., Bebout and Penniston-Dorland, 2016) and further dedicated investigations are required. Together with high-*P* serpentinites, subducted Mg-Al rich oceanic crust could act as a reservoir of B with a heavy isotope signature (i.e., with positive δ^{11}B), with a sizeable contribution to the global B cycle.

7. Concluding remarks

Metamafic rocks from the Voltri Unit were investigated for their major and trace element composition and δ^{11}B, δ^{18}O and Sr isotope signatures and the main results of our study can be summarized as follows:

- Oxygen isotope compositions and ^{87}Sr/^{86}Sr ratios of metamafic rocks from the Voltri Massif mainly reflect inherited signatures from the seafloor, whereas subduction-related processes are mainly traced through δ^{11}B variations.
- Progressive B isotope fractionation due to subduction-zone dehydration are responsible for the dominant negative δ^{11}B signatures of eclogites from the Vara area, whereas the ^{11}B-rich

imprint of the high-*P* metarodingite is compatible with inheritance of the oceanic signatures, although an interaction with fluids released by the surrounding serpentinites at peak conditions cannot be ruled out.

- The Erro-Tobbio eclogite shows enrichment in Li/Y and B/Nb ratios and positive $\delta^{11}B$ signature: to our knowledge, this is the first report worldwide. Three scenarios are evaluated: (i) inheritance of oceanic signatures, (ii) record of B isotope fractionation from an extreme ^{11}B-rich protolith, or (iii) interaction with ^{11}B-rich slab fluids during hydration at high-*P* conditions.
- We propose that the protolith composition of the mafic crust controls the development of hydrous phases at high-*P* thus enabling the storage of ^{11}B. Although further *in-situ* $\delta^{11}B$ investigations are required, we claim that this mechanism of chemical transfer may generate a ^{11}B-rich reservoir that, along with high-P serpentinites, will provide positive $\delta^{11}B$ domains in the mantle.

Acknowledges

L. Federico (University of Genova) is acknowledged for providing sample FL4. EC thanks L. Crispini (University of Genova) for stimulating discussion about the Vara area and S. Tumiati (University of Milano) for advice on thermodynamic calculations. Magnani L. and Sessa G. (University of Milano) are acknowledged for support during pellets preparation and LA-ICP-MS analyses, respectively. The trace element work benefits funding from the Italian Ministry of Education, University and Research (MIUR) – Excellent Departments Projects. Boron and Sr isotope analyses were partially supported by IGG-CNR fund P1600514 to SA. MS acknowledges the Italian MUR for granting the PRIN project Dynastars (2017ZE49E7). Constructive reviews by W.P. Leeman and an anonymous reviewer, and editorial handling by Editor B. Kamber, greatly improved the presentation of the manuscript and are much appreciated.

Figure captions

Figure 1. Simplified geological map of the Voltri Massif and surrounding Units (modified from Capponi et al., 2016). Locations of the collected samples are indicated with the yellow stars.

Figure 2. Microphotographs of the eclogitized metamafic rocks from Vara. **(A)** Mylonitic foliation of sample ENV1 made of omphacite 2 (omp2) + garnet (grt) + rutile (rt) surrounding syn-deformed porphyroblast of omphacite 1 (omp1). Locally are present retrogression of glaucophanic amphibole (gln) and symplectites (sympl). **(B)** Sample ENV10/2, showing garnet-rich layer with omphacite 2 and rutile. **(C)** high-*P* vein made of garnet and limpid diopside (di2) crosscutting prograde diopside (di1) grains from the metarodiginte sample ENV11B.

Figure 3. N-MORB normalized (Sun and McDonough, 1989; reference values for B and Li are from Marschall et al., 2017) Rare Earth Element (REE) and trace element patterns for Vara **(A, C)** and Erro-Tobbio **(B, D)** metamafic rocks. In (A) the light green field reports the range of oxide gabbros from the IODP site U1309 (Godard et al., 2009), whereas in (B) the light purple field reports the range of olivine gabbros from the IODP site U1309 (Godard et al., 2009). In (B) are also reported the REE patterns of unmetamorphosed troctolite and olivine-gabbros from the Erro-Tobbio (small grey circles, Borghini et al., 2007).

Figure 4. Boron concentrations, $\delta^{11}B$, $\delta^{18}O$ and $^{87}Sr/^{86}Sr$ isotope compositions of the eclogitized metamafic rocks from the Voltri Unit (green and purple symbols: Vara and Erro-Tobbio samples, respectively): **(A)** B (ppm) *vs.* $\delta^{11}B$ (‰); **(A)** $\delta^{18}O$ (‰) *vs.* $\delta^{11}B$ (‰); **(C)** $\delta^{18}O$ (‰) *vs.* B (ppm); **(D)** $\delta^{11}B$ (‰) *vs.* $^{87}Sr/^{86}Sr$. Data for variably altered gabbros from the Troodos, Oman and N. Apennines ophiolites, the altered oceanic crust (AOC) and mantle-MORB are reported for comparison (Marschall et al., 2017; Mattey et al., 1994; Schwarzenbach et al., 2021; Smith et al., 1995; Yamaoka et al., 2015, 2012).

Figure 5. Fluid-mobile (Li, B, Sr, Ba) *vs.* fluid-immobile (Nd, Nb, Y) element ratios for the Voltri eclogites and metarodingite (legend as in Fig. 3). The dashed purple field reports the range of olivine gabbros from the IODP site U1309 (Godard et al., 2009), whereas the light green contour reports the range of oxide gabbros from the IODP site U1309 (Godard et al., 2009). Small gray circles are unmetamorphosed troctolite and olivine-gabbros from the Erro-Tobbio (Borghini et al., 2007). N-MORB value from Sun and McDonough (1989) and Marschall et al. (2017). Legend as in **Fig. 3**.

Figure 6. (A) P-X_{H2O} isothermal (T = 550 °C) and **(B)** T-X_{H2O} isobaric (P =2.5 GPa) pseudosections calculated in the NCFMAS-H_2O system for the olivine-bearing gabbros as the oceanic equivalent of the Erro-Tobbio eclogites. Yellow fields represent the high-P mineral assemblages for the Erro-Tobbio eclogites. Mineral abbreviations: gt: garnet; cpx: clinopyroxene; zo: zoisite; t: talc; law: lawsonite; ctd: chloritoid; chl: chlorite; ky: kyanite; q: quartz; amph: amphibole; coe: coesite.

Figure 7. Boron concentration (in ppm) *vs.* $\delta^{11}B$ (‰) of the Voltri eclogitized metamafic rocks compared with several subducted-derived high-P mafic rocks and minerals. Whole-rock data of lawsonite-blueschist matrix melange of the Catalina Schist are from King et al. (2007); amphibole and phengite from the Mariana forearc blueschist mafic rocks are from(Pabst et al., 2012); ranges for the metasomatized tourmaline from Syros and for the restitic slab are from Marschall et al. (2006) and Peacock and Hervig (1999), respectively (see text for discussion). Legend as in **Fig. 3**.

Figure 8. Eu_N/Eu^*_N *vs.* Li/Y**(A)** and B/Nb **(B)** ratios for the Voltri eclogites and metarodingite (legend as in **Fig. 3**). The positive correlation shown by the Erro-Tobbio eclogites suggests the dependence of the igneous plagioclase alteration by fluids and the enrichment in Li and B. The dashed purple field reports the range of olivine gabbros from the IODP site U1309 (Godard et al., 2009),

whereas the light green contour reports the range of oxide gabbros from the IODP site U1309 (Godard et al., 2009). N-MORB value from Sun and McDonough (1989) and Marschall et al. (2017).

Figure 9. Schematic 1D-diagrams showing the main relationship between H_2O (wt.%) and B (ppm) contents (in blue and green, respectively) and $\delta^{11}B$ (‰; in red) for Mg-Al gabbros at the oceanic and high-*P* stages (at 160 and 40(?) Ma, respectively). Three major scenarios are reported: oceanic inheritance and internal element re-distribution **(A)**, partial dehydration associated with B release and B isotope fractionation **(B)**, and interaction with ^{11}B-rich fluids overprinting scenario 1 and 2 **(C)**. Oceanic H_2O data (n = 109) are from Godard et al. (2009) and Kendrick (2019); B and $\delta^{11}B$ data (n = 48) are from Smith et al. (1995), Yamaoka et al. (2012, 2015) and McCaig et al. (2018). High-*P* boxes represent the range of the Erro-Tobbio eclogites from in this study. For oceanic data: error bars are maximum and minimum values of data population; each box refers to 10^{th} and 90^{th} percentile of the data population while the black line within the box is the mean of the data population.

References

Agostini, S., di Giuseppe, P., Manetti, P., Doglioni, C., Conticelli, S., 2021. A heterogeneous subcontinental mantle under the African–Arabian Plate boundary revealed by boron and radiogenic isotopes. Sci Rep 11. https://doi.org/10.1038/s41598-021-90275-7

Agostini, S., di Giuseppe, P., Manetti, P., Savaşçın, M.Y., Conticelli, S., 2022. Geochemical and isotopic (Sr-Nd-Pb) signature of crustal contamination in Na-alkali basaltic magmas of South-East Turkey. Italian Journal of Geosciences 141, 363–384. https://doi.org/10.3301/IJG.2022.21

Alt, J.C., Shanks, W.C., Crispini, L., Gaggero, L., Schwarzenbach, E.M., Früh-Green, G.L., Bernasconi, S.M., 2012. Uptake of carbon and sulfur during seafloor serpentinization and the effects of subduction metamorphism in Ligurian peridotites. Chem Geol 322–323, 268–277. https://doi.org/10.1016/j.chemgeo.2012.07.009

Angiboust, S., Langdon, R., Agard, P., Waters, D., Chopin, C., 2012. Eclogitization of the Monviso ophiolite (W. Alps) and implications on subduction dynamics. Journal of Metamorphic Geology 30, 37–61. https://doi.org/10.1111/j.1525-1314.2011.00951.x

Bach, W., Klein, F., 2009. The petrology of seafloor rodingites: Insights from geochemical reaction path modeling. Lithos 112, 103–117. https://doi.org/10.1016/j.lithos.2008.10.022

Barnes, J.D., Beltrando, M., Lee, C.T.A., Cisneros, M., Loewy, S., Chin, E., 2014. Geochemistry of Alpine serpentinites from rifting to subduction: A view across paleogeographic domains and metamorphic grade. Chem Geol 389, 29–47. https://doi.org/10.1016/j.chemgeo.2014.09.012

Barnicoat, A.C., Cartwright, I., 1997. The gabbro-eclogite transformation: an oxygen isotope and petrographic study of west Alpine ophiolites. Journal of Metamorphi Geology 15, 93–104.

Bebout, G.E., Nakamura, E., 2003. Record in metamorphic tourmalines of subduction-zone devolatilization and boron cycling, Geology

Bebout, G.E., Penniston-Dorland, S.C., 2015. Fluid and mass transfer at subduction interfaces-The field metamorphic record. Lithos. https://doi.org/10.1016/j.lithos.2015.10.007

Benton, L.D., Ryan, J.G., Tera, F., 2001. Boron isotope systematics of slab fluids as inferred from a serpentine seamount, Mariana forearc. Earth Planet Sci Lett 187, 273–282.

Bocchio, R., 1995. Chemical variations in clinopyroxene and garnet from eclogites of the Vara Valley (Voltri Group, Italy). European Journal of Mineralogy 7, 103–118. https://doi.org/10.1127/ejm/7/1/0103

Borghini, G., Rampone, E., Crispini, L., de Ferrari, R., Godard, M., 2007. Origin and emplacement of ultramafic–mafic intrusions in the Erro-Tobbio mantle peridotite (Ligurian Alps, Italy). Lithos 94, 210–229. https://doi.org/10.1016/j.lithos.2006.06.014

Brouwer, F.M., Vissers, R.L.M., Lamb, W.M., 2002. Metamorphic history of eclogitic metagabbro blocks from a tectonic mélange in the Voltri Massif, Ligurian Alps, Italy. Ofioliti 27, 1–16.

Cannaò, E., 2020. Boron isotope fractionation in subducted serpentinites: A modelling attempt. Lithos 376–377. https://doi.org/10.1016/j.lithos.2020.105768

Cannaò, E., Agostini, S., Scambelluri, M., Tonarini, S., Godard, M., 2015. B, Sr and Pb isotope geochemistry of high-pressure Alpine metaperidotites monitors fluid-mediated element recycling during serpentinite dehydration in subduction mélange (Cima di Gagnone, Swiss Central Alps). Geochim Cosmochim Acta 163. https://doi.org/10.1016/j.gca.2015.04.024

Cannaò, E., Malaspina, N., 2018. From oceanic to continental subduction: Implications for the geochemical and redox evolution of the supra-subduction mantle. Geosphere 14. https://doi.org/10.1130/GES01597.1

Cannaò, E., Scambelluri, M., Agostini, S., Tonarini, S., Godard, M., 2016. Linking serpentinite geochemistry with tectonic evolution at the subduction plate interface: The Voltri Massif case study (Ligurian Western Alps, Italy). Geochim Cosmochim Acta 190. https://doi.org/10.1016/j.gca.2016.06.034

Capponi, G., Crispini, L., Federico, L., Malatesta, C., 2016. Geology of the eastern ligurian alps: A review of the tectonic units. Italian Journal of Geosciences 135, 157–169. https://doi.org/10.3301/IJG.2015.06

Cartwright, I., Barnicoat, A.C., 1999. Stable isotope geochemistry of Alpine ophiolites: a window to ocean-floor hydrothermal alteration and constraints on fluid-rock interaction during high-pressure metamorphism. Int Journ Earth Sciences. Springer-Verlag.

Chiesa, S., Cortesogno, L., Forcella, F., Galli, M., Messiga, B., Pasquaré, G., Pedemonte, G.M., Piccardo, G.B., Rossi, P.M., 1975. Assetto strutturale ed interpretazione geodinamica del Gruppo di Voltri. Bollettino Società Geologica Italiana 94, 555–581.

Cimmino, F., Messiga, B., Piccardo, G.B., 1981. Le carateristiche paragenetiche dell'evento di alta-pressione nei diffrenti sistemi (pelitici, femici, ultrafemici) delle ofioliti metamorfiche del Gruppo di Voltri (Liguria Occidentale). Rendiconti della Societàà Geologica Italiana di Mineralogia e Petrografia 37, 419–446.

Clarke, E., de Hoog, J.C.M., Kirstein, L.A., Harvey, J., Debret, B., 2020. Metamorphic olivine records external fluid infiltration during serpentinite dehydration. Geochem Perspect Lett 16, 25–29. https://doi.org/10.7185/GEOCHEMLET.2039

Connolly, J.A.D., 2005. Computation of phase equilibria by linear programming: A tool for geodynamic modeling and its application to subduction zone decarbonation. Earth Planet Sci Lett 236, 524–541. https://doi.org/10.1016/j.epsl.2005.04.033

Cortesogno, L., Ernst, W.G., Galli, M., Messiga, B., Pedemonte, G.M., Piccardo, G.B., 1977. Chemical Petrology of Eclogitic Lenses in Serpentinite, Gruppo di Voltri, Ligurian Alps. J Geol. https://doi.org/10.1086/628298

Crispini, L., Capponi, G., 2007. Tectonic evolution of the Voltri Group and Sestri Voltaggio Zone (southern limit of the NW Alps): a review. Ofioliti 26, 161–164.

de Hoog, J.C.M., Savov, I.P., 2018. Boron Isotopes as a Tracer of Subduction Zone Processes, in: Marschall Horst and Foster, G. (Ed.), Boron Isotopes: The Fifth Element. Springer International Publishing, Cham, pp. 217–247. https://doi.org/10.1007/978-3-319-64666-4_9

Dick, H.J.B., Natland, J.H., Alt, J.C., Bach, W., Bideau, D., Gee, J.S., Haggas, S., Hertogen, J.G.H., Hirth, G., Holm, P.M., Ildefonse, B., Iturrino, G.J., John, B.E., Kelley, D.S., Kikawa, E., Kingdon, A., Leroux, P.J., Maeda, J., Meyer, P.S., Miller, D.J., Naslund, H.R., Niu, Y.-L., Robinson, P.T., Snow, J., Stephen, R.A., Trimby, P.W., Worm, H.-U., Yoshinobu, A., 2000. A long in situ section of the lower ocean crust: results of ODP Leg 176 drilling at the Southwest Indian Ridge. Earth Planet Sci Lett 179, 31–51.

Evans, B.W., Trommsdorff, V., Richter, W., 1979. Petrology of an eclogite-metarodingite suite at Cima di Gagnone, Ticino, Switzerland. American Mineralogist 64, 15–31.

Federico, L., Capponi, G., Crispini, L., Scambelluri, M., Villa, I.M., 2005. 39Ar/40Ar dating of high-pressure rocks from the Ligurian Alps: Evidence for a continuous subduction-exhumation cycle. Earth Planet Sci Lett 240, 668–680. https://doi.org/10.1016/j.epsl.2005.09.062

Federico, L., Crispini, L., Scambelluri, M., Capponi, G., 2007. Ophiolite mélange zone records exhumation in a fossil subduction channel. Geology 35, 499. https://doi.org/10.1130/G23190A.1

Ferrando, C., France, L., Basch, V., Sanfilippo, A., Tribuzio, R., Boulanger, M., 2021. Grain Size Variations Record Segregation of Residual Melts in Slow-Spreading Oceanic Crust (Atlantis Bank, 57°E Southwest Indian Ridge). J Geophys Res Solid Earth 126. https://doi.org/10.1029/2020JB020997

Früh-Green, G.L., Scambelluri, M., Vallis, F., 2001. O-H isotope ratios of high pressure ultramafic rocks: Implications for fluid sources and mobility in the subducted hydrous mantle. Contributions to Mineralogy and Petrology 141, 145–159. https://doi.org/10.1007/s004100000228

Gillis, K.M., Snow, J.E., Klaus, A., Abe, N., Adrião, A.B., Akizawa, N., Ceuleneer, G., Cheadle, M.J., Faak, K., Falloon, T.J., Friedman, S.A., Godard, M., Guerin, G., Harigane, Y., Horst, A.J., Hoshide, T., Ildefonse, B., Jean, M.M., John, B.E., Koepke, J., MacHi, S., Maeda, J., Marks, N.E., McCaig, A.M., Meyer, R., Morris, A., Nozaka, T., Python, M., Saha, A., Wintsch, R.P., 2014. Primitive layered gabbros from fast-spreading lower oceanic crust. Nature 505, 204–207. https://doi.org/10.1038/nature12778

Godard, M., Awaji, S., Hansen, H., Hellebrand, E., Brunelli, D., Johnson, K., Yamasaki, T., Maeda, J., Abratis, M., Christie, D., Kato, Y., Mariet, C., Rosner, M., 2009. Geochemistry of a long in-situ section of intrusive slow-spread oceanic lithosphere: Results from IODP Site U1309 (Atlantis Massif, 30°N Mid-Atlantic-Ridge). Earth Planet Sci Lett 279, 110–122. https://doi.org/10.1016/j.epsl.2008.12.034

Hacker, B.R., 2008. H2O subduction beyond arcs. Geochemistry, Geophysics, Geosystems 9. https://doi.org/10.1029/2007GC001707

Halama, R., Konrad-Schmolke, M., de Hoog, J.C.M., 2020. Boron isotope record of peak metamorphic ultrahigh-pressure and retrograde fluid–rock interaction in white mica (Lago di

Cignana, Western Alps). Contributions to Mineralogy and Petrology 175. https://doi.org/10.1007/s00410-020-1661-8

Haws, A.A., Starr, P.G., Dragovic, B., Scambelluri, M., Belmonte, D., Caddick, M.J., Broadwell, K.S., Ague, J.J., Baxter, E.F., 2021. Meta-rodingite dikes as recorders of subduction zone metamorphism and serpentinite dehydration: Voltri Ophiolite, Italy. Chem Geol 565. https://doi.org/10.1016/j.chemgeo.2021.120077

Hermann, J., Zheng, Y.F., Rubatto, D., 2013. Deep fluids in subducted continental crust. Elements 9, 281–287. https://doi.org/10.2113/gselements.9.4.281

Kendrick, M.A., 2019. Halogens in Atlantis Bank gabbros, SW Indian Ridge: Implications for styles of seafloor alteration. Earth Planet Sci Lett 514, 96–107. https://doi.org/10.1016/j.epsl.2019.02.034

King, R.L., Bebout, G.E., Grove, M., Moriguti, T., Nakamura, E., 2007. Boron and lead isotope signatures of subduction-zone mélange formation: Hybridization and fractionation along the slab-mantle interface beneath volcanic arcs. Chem Geol 239, 305–322. https://doi.org/10.1016/j.chemgeo.2007.01.009

Konrad-Schmolke, M., Halama, R., 2014. Combined thermodynamic–geochemical modeling in metamorphic geology: Boron as tracer of fluid–rock interaction. Lithos 208–209, 393–414. https://doi.org/10.1016/j.lithos.2014.09.021

Laborda-López, C., López-Sánchez-Vizcaíno, V., Marchesi, C., Gómez-Pugnaire, M.T., Garrido, C.J., Jabaloy-Sánchez, A., Padrón-Navarta, J.A., Hidas, K., 2018. High-P metamorphism of rodingites during serpentinite dehydration (Cerro del Almirez, Southern Spain): Implications for the redox state in subduction zones. Journal of Metamorphic Geology 36, 1141–1173. https://doi.org/10.1111/jmg.12440

Laborda-López, C., Marchesi, C., López Sánchez-Vizcaíno, V., Gómez-Pugnaire, M.T., Dale, C.W., Jabaloy-Sánchez, A., Padrón-Navarta, J.A., Román-Alpiste, M.J., Garrido, C.J., 2020.

Geochemical evolution of rodingites during subduction: insights from Cerro del Almirez (southern Spain). Lithos 370–371. https://doi.org/10.1016/j.lithos.2020.105639

Lafay, R., Baumgartner, L.P., Putlitz, B., Siron, G., 2019. Oxygen isotope disequilibrium during serpentinite dehydration. Terra Nova 31, 94–101. https://doi.org/10.1111/ter.12373

Leeman, W.P., Sisson, V.B., 1996. Chapter 12. GEOCHEMISTRY OF BORON AND ITS IMPLICATIONS FOR CRUSTAL AND MANTLE PROCESSES, in: Boron. De Gruyter, pp. 645–708. https://doi.org/10.1515/9781501509223-014

Liou, J., Zhang, R., Ernst, W., Liu, J., Mclimans, R., 1998. Mineral parageneses in the Piampaludo eclogitic body, Gruppo di Voltri, Western Ligurian Alps . Schweiz. Mineral. Petrogr. Mitt. 78, 317–335.

Malatesta, C., Crispini, L., Federico, L., Capponi, G., Scambelluri, M., 2012. The exhumation of high pressure ophiolites (Voltri Massif, Western Alps): Insights from structural and petrologic data on metagabbro bodies. Tectonophysics 568–569, 102–123. https://doi.org/10.1016/j.tecto.2011.03.024

Mallik, A., Li, Y., Wiedenbeck, M., 2018. Nitrogen evolution within the Earth's atmosphere–mantle system assessed by recycling in subduction zones. Earth Planet Sci Lett 482, 556–566. https://doi.org/10.1016/j.epsl.2017.11.045

Marschall, H.R., Ludwig, T., Altherr, R., Kalt, A., Tonarini, S., 2006. Syros metasomatic tourmaline: Evidence for very high-δ11 B fluids in subduction zones. Journal of Petrology 47, 1915–1942. https://doi.org/10.1093/petrology/egl031

Marschall, H.R., Wanless, V.D., Shimizu, N., Pogge von Strandmann, P.A.E., Elliott, T., Monteleone, B.D., 2017. The boron and lithium isotopic composition of mid-ocean ridge basalts and the mantle. Geochim Cosmochim Acta 207, 102–138. https://doi.org/10.1016/j.gca.2017.03.028

Martin, C., Flores, K.E., Harlow, G.E., 2016. Boron isotopic discrimination for subduction-related serpentinites. Geology 44, 899–902. https://doi.org/10.1130/G38102.1

Mattey, D., Lowry, D., Macpherson, C., 1994. Oxygen isotope composition of mantle peridotite. Earth Planet Sci Lett 128, 231–241.

Mcarthur, J.M., Howarth, R.J., Bailey, T.R., 2001. Strontium Isotope Stratigraphy: LOWESS Version 3: Best Fit to the Marine Sr-Isotope Curve for 0-509 Ma and Accompanying Look-up Table for Deriving Numerical Age, The Journal of Geology.

McCaig, A.M., Titarenko, S.S., Savov, I.P., Cliff, R.A., Banks, D., Boyce, A., Agostini, S., 2018. No significant boron in the hydrated mantle of most subducting slabs. Nat Commun 9. https://doi.org/10.1038/s41467-018-07064-6

Messiga, B., Piccardo, G.B., Ernst, W.G., 1983. High-pressure Eo-Alpine parageneses developed in magnesian metagabbros, Gruppo di Voltri, Western Liguria, Italy. Contributions to Mineralogy and Petrology. https://doi.org/10.1007/BF00373074

Messiga, B., Scambelluri, M., 1991. Retrograde P-T path for the Voltri Massif eclogites (Ligurian Alps, Italy): some tectonic implications. Journal of Metamorphic Geology 9, 93–109.

Messiga, B., Scambelluri, M., Piccardo, G.B., 1995. CHLORITOID-BEARING ASSEMBLAGES IN MAFIC SYSTEMS AND ECLOGITE-FACIES HYDRATION OF ALPINE MG-AL METAGABBROS (ERRO-TOBBIO UNIT, LIGURIAN WESTERN ALPS). European Journal of Mineralogy 7, 1149–1167.

Pabst, S., Zack, T., Savov, I.P., Ludwig, T., Rost, D., Tonarini, S., Vicenzi, E.P., 2012. The fate of subducted oceanic slabs in the shallow mantle: Insights from boron isotopes and light element composition of metasomatized blueschists from the Mariana forearc. Lithos 132–133, 162–179. https://doi.org/10.1016/j.lithos.2011.11.010

Peacock, S.M., 1993. The importance of blueschist-» eclogite dehydration reactions in subducting oceanic crust. Geol Soc Am Bull 105, 689–694.

Peacock, S.M., Hervig, R.L., 1999. Boron isotopic composition of subduction-zone metamorphic rocks, Chemical Geology.

Pelletier, L., Müntener, O., 2006. High-pressure metamorphism of the Lanzo peridotite and its oceanic cover, and some consequences for the Sesia-Lanzo zone (northwestern Italian Alps). Lithos 90, 111–130. https://doi.org/10.1016/j.lithos.2006.01.006

Plank, T., Manning, C.E., 2019. Subducting carbon. Nature. https://doi.org/10.1038/s41586-019-1643-z

Plümper, O., John, T., Podladchikov, Y.Y., Vrijmoed, J.C., Scambelluri, M., 2017. Fluid escape from subduction zones controlled by channel-forming reactive porosity. Nat Geosci 10, 150–156. https://doi.org/10.1038/ngeo2865

Poli, S., 1995. The amphibolite-eclogite transformation: an experimental study on basalt. Am J Sci 293, 1061–1107.

Poli, S., Schmidt, M.W., 1997. The high-pressure stability of hydrous phases in orogenic belts: an experimental approach on eclogite-forming processes, Tectonophysics.

Poli, S., Schmidt, M.W., 1995. H2O transport and release in subduction zones: experimental constraints on basaltic and andesitic systems. J Geophys Res 100. https://doi.org/10.1029/95jb01570

Prigent, C., Guillot, S., Agard, P., Lemarchand, D., Soret, M., Ulrich, M., 2018. Transfer of subduction fluids into the deforming mantle wedge during nascent subduction: Evidence from trace elements and boron isotopes (Semail ophiolite, Oman). Earth Planet Sci Lett 484, 213–228. https://doi.org/10.1016/j.epsl.2017.12.008

Putlitz, B., Matthews, A., Valley, J.W., 2000. Oxygen and hydrogen isotope study of high-pressure metagabbros and metabasalts (Cyclades, Greece): implications for the subduction of oceanic crust. Contribution to Mineralogy and Petrology 114–126.

Rosner, M., Erzinger, J., Franz, G., Trumbull, R.B., 2003. Slab-derived boron isotope signatures in arc volcanic rocks from the Central Andes and evidence for boron isotope fractionation during progressive slab dehydration. Geochemistry, Geophysics, Geosystems 4. https://doi.org/10.1029/2002GC000438

Rubatto, D., Scambelluri, M., 2003. U-Pb dating of magmatic zircon and metamorphic baddeleyite in the Ligurian eclogites (Voltri Massif, Western Alps). Contributions to Mineralogy and Petrology 146, 341–355. https://doi.org/10.1007/s00410-003-0502-x

Rüpke, L.H., Morgan, J.P., Hort, M., Connolly, J.A.D., 2004. Serpentine and the subduction zone water cycle. Earth Planet Sci Lett 223, 17–34. https://doi.org/10.1016/j.epsl.2004.04.018

Savov, I.P., Ryan, J.G., D'Antonio, M., Kelley, K., Mattie, P., 2005. Geochemistry of serpentinized peridotites from the Mariana Forearc Conical Seamount, ODP Leg 125: Implications for the elemental recycling at subduction zones. Geochemistry, Geophysics, Geosystems 6. https://doi.org/10.1029/2004GC000777

Scambelluri, M., Bebout, G.E., Belmonte, D., Gilio, M., Campomenosi, N., Collins, N., Crispini, L., 2016. Carbonation of subduction-zone serpentinite (high-pressure ophicarbonate ; Ligurian Western Alps) and implications for the deep carbon cycling. Earth Planet Sci Lett 441, 155–166. https://doi.org/10.1016/j.epsl.2016.02.034

Scambelluri, M., Bottazzi, P., Trommsdorff, V., Vannucci, R., Hermann, J., Gòmez-Pugnaire, M.T., Lòpez-Sànchez Vizcano, V., 2001. Incompatible element-rich fluids released by antigorite breakdown in deeply subducted mantle. Earth Planet Sci Lett 192, 457–470. https://doi.org/10.1016/S0012-821X(01)00457-5

Scambelluri, M., Cannaò, E., Gilio, M., 2019. The water and fluid-mobile element cycles during serpentinite subduction. A review. European Journal of Mineralogy 31. https://doi.org/10.1127/ejm/2019/0031-2842

Scambelluri, M., Hoogerduijn Strating, E.H., Piccardo, G.B., Vissers, R.L.M., Rampone, E., 1991. Alpine olivine- and titanian clinohumite-bearing assemblages in the Erro-Tobbio peridotite (Voltri Massif, NW Italy). Journal of Metamorphic Geology 9, 79–91. https://doi.org/10.1111/j.1525-1314.1991.tb00505.x

Scambelluri, M., Müntener, O., Hermann, J., Piccardo, G.B., Trommsdorff, V., 1995. Subduction of water into the mantle: History of an Alpine peridotite. Geology 23, 459–462.

Scambelluri, M., Pettke, T., Cannaò, E., 2015. Fluid-related inclusions in Alpine high-pressure peridotite reveal trace element recycling during subduction-zone dehydration of serpentinized mantle (Cima di Gagnone, Swiss Alps). Earth Planet Sci Lett 429. https://doi.org/10.1016/j.epsl.2015.07.060

Scambelluri, M., Rampone, E., 1999. Mg-metasomatism of oceanic gabbros and its control on Ti-clinohumite formation during eclogitization. Contributions to Mineralogy and Petrology.

Scambelluri, M., Tonarini, S., 2012. Boron isotope evidence for shallow fluid transfer across subduction zones by serpentinized mantle. Geology 40, 907–910. https://doi.org/10.1130/G33233.1

Scarsi, M., Malatesta, C., Fornasaro, S., 2017. Lawsonite-bearing eclogite from a tectonic mélange in the Ligurian Alps: New constraints for the subduction plate-interface evolution. Geol Mag 155, 280–297. https://doi.org/10.1017/S0016756817000395

Schmidt, M.W., Poli, S., 2014. Devolatilization During Subduction, in: Treatise on Geochemistry. Elsevier, pp. 669–701. https://doi.org/10.1016/B978-0-08-095975-7.00321-1

Schwarzenbach, E.M., Vogel, M., Früh-Green, G.L., Boschi, C., 2021. Serpentinization, Carbonation, and Metasomatism of Ultramafic Sequences in the Northern Apennine Ophiolite (NW Italy). J Geophys Res Solid Earth 126. https://doi.org/10.1029/2020JB020619

Smith, H.J., Spivack, A.J., Staudigel, H., Hart, S.R., 1995. The boron isotopic composition of altered oceanic crust. Chem Geol 126, 119–135.

Spandler, C., Hermann, J., Arculus, R., Mavrogenes, J., 2003. Redistribution of trace elements during prograde metamorphism from lawsonite blueschist to eclogite facies; implications for deep subduction-zone processes. Contributions to Mineralogy and Petrology 146, 205–222. https://doi.org/10.1007/s00410-003-0495-5

Spandler, C., Pettke, T., Hermann, J., 2014. Experimental study of trace element release during ultrahigh-pressure serpentinite dehydration. Earth Planet Sci Lett 391, 296–306. https://doi.org/10.1016/j.epsl.2014.02.010

Starr, P.G., Broadwell, K.S., Dragovic, B., Scambelluri, M., Haws, A.A., Caddick, M.J., Smye, A.J., Baxter, E.F., 2020. The subduction and exhumation history of the Voltri Ophiolite, Italy: Evaluating exhumation mechanisms for high-pressure metamorphic massifs. Lithos 376–377. https://doi.org/10.1016/j.lithos.2020.105767

Staudigel, H., 2014. Chemical Fluxes from Hydrothermal Alteration of the Oceanic Crust, in: Treatise on Geochemistry. Elsevier, pp. 583–606. https://doi.org/10.1016/B978-0-08-095975-7.00318-1

Straub, S.M., Layne, G.D., 2003. Decoupling of fluids and fluid-mobile elements during shallow subduction: Evidence from halogen-rich andesite melt inclusions from the Izu arc volcanic front. Geochemistry, Geophysics, Geosystems 4. https://doi.org/10.1029/2002GC000349

Sun, S., McDonough, W.F., 1989. Chemical and isotopic systematics of oceanic basalts: implications for mantle composition and processes. Geol Soc Spec Publ 313–345.

Tonarini, S., Leeman, W.P., Leat, P.T., 2011. Subduction erosion of forearc mantle wedge implicated in the genesis of the South Sandwich Island (SSI) arc: Evidence from boron isotope systematics. Earth Planet Sci Lett 301, 275–284. https://doi.org/10.1016/j.epsl.2010.11.008

Vignaroli, G., Rossetti, F., Bouybaouene, M., Massonne, H.-J., Theye, T., Faccenna, C., Funiciello, R., 2005. A counter-clockwise P--T path for the Voltri Massif eclogites (Ligurian Alps, Italy). Journal of Metamorphic Geology 23, 533–555.

Vignaroli, G., Rossetti, F., Rubatto, D., Theye, T., Lisker, F., Phillips, D., 2010. Pressure-temperature-deformation-time (P-T-d-t) exhumation history of the Voltri Massif HP complex, Ligurian Alps, Italy. Tectonics 29. https://doi.org/10.1029/2009TC002621

Wenner, D.B., Taylor, H.P., 1971. Temperatures of Serpentinization of Ulramafic Rocks Based on O18/O16 Fractionation between Coexisting Serpentine and Magnetite. Contr. Mineral. and Petrol 32, 165–185.

Wilson, D.S., H Teagle, D.A., Alt, J.C., Banerjee, N.R., Umino, S., Miyashita, S., Acton, G.D., Anma, R., Barr, S.R., Belghoul, A., Carlut, J., Christie, D.M., Coggon, R.M., Cooper, K.M.,

Cordier, C., Crispini, L., Rodriguez Durand, S., Einaudi, F., Galli, L., Gao, Y., Geldmacher, J., Gilbert, L.A., Hayman, N.W., Herrero-Bervera, E., Hirano, N., Holter, S., Ingle, S., Jiang, S., Kalberkamp, U., Kerneklian, M., rgen Koepke, J., Laverne, C., Lledo Vasquez, H.L., Maclennan, J., Morgan, S., Neo, N., Nichols, H.J., Park, S.-H., Reichow, M.K., Sakuyama, T., Sano, T., Sandwell, R., Scheibner, B., Smith-Duque, C.E., Swift, S.A., Tartarotti, P., Tikku, A.A., Tominaga, M., Veloso, E.A., Yamasaki, T., Yamazaki, S., Ziegler, C., 2006. Drilling to Gabbro in Intact Ocean Crust. Science (1979) 312, 1016–1020.

Yamaoka, K., Ishikawa, T., Matsubaya, O., Ishiyama, D., Nagaishi, K., Hiroyasu, Y., Chiba, H., Kawahata, H., 2012. Boron and oxygen isotope systematics for a complete section of oceanic crustal rocks in the Oman ophiolite. Geochim Cosmochim Acta 84, 543–559. https://doi.org/10.1016/j.gca.2012.01.043

Yamaoka, K., Matsukura, S., Ishikawa, T., Kawahata, H., 2015. Boron isotope systematics of a fossil hydrothermal system from the Troodos ophiolite, Cyprus: Water-rock interactions in the oceanic crust and subseafloor ore deposits. Chem Geol 396, 61–73. https://doi.org/10.1016/j.chemgeo.2014.12.023

Zanoni, D., Rebay, G., Spalla, M.I., 2016. Ocean floor and subduction record in the Zermatt-Saas rodingites, Valtournanche, Western Alps. Journal of Metamorphic Geology 34, 941–961. https://doi.org/10.1111/jmg.12215

Table 1. Summary of petrographic information for individual samples and main mineral assemblages

Area	Lithology	Sample	Texture	Relict of magmatic assemblage	Eclogite peak assemblage		Post-eclogitic assemblage
					Main domains	*Coronas*	
Vara	Fe-Ti metagabbro	**ENV1**	*Foliated*	-	omph + grt + rt ± qtz	-	gln ± di ± act
		ENV10/2	*Foliated*	-	omph + grt + rt ± qtz	-	gln
		FL4	*Foliated*	-	omph + grt + rt ± qtz	-	gln ± di ± act
	Metarodingite	**ENV11B**	*Massive*	di	di + grt + chl	-	
Erro-Tobbio	Mg-Al metagabbro	**MG5**	*Coronitic*	aug, ol	omph + tl + jd + zo + grt + chl ± qtz	di + chl / tl + ctl + grt	gln + chl + pg + mrg
		F1	*Coronitic*	aug, ol	omph + tl + jd + zo + grt + chl ± qtz	tl + clt + grt	gln + chl + pg + mrg
		MG4/7	*Coronitic*	aug, ol	omph + tl + jd + zo + grt + chl + opx ± qtz	chl + grt / tl + clt + grt	gln + chl + pg + mrg
		E89-26	*Foliated*	-	omph + grt + chl + jd + zo + qtz + ctl + tl	-	gln + chl + pg + mrg

Omph: omphacite; grt: garnet; rt: rutile; gln: glaucophane; di: diopside; chl: chlorite; aug: augite; ol: olivine; tl: talc; jd: jadeite; zo: zoisite; clt: clorithoid; qtz: quartz; opx: orthopyroxene; pg: paragonite; mrg: margarite

Table 2. Major (wt.%) and trace element (µg/g) composition of the studied metamafic rocks

Vara - Fe-Ti metagabbro						*Vara - Metarodingite*	*Erro-Tobbio - Mg-Al metagabbro*							
ENV1		**ENV10/2**		**FL4**		**ENV11b**	**MG5**		**F1**		**MG4/7**		**E89-26**	
R	S	R	S	R	S	RSD	R	S	R	S	R	S	R	S
D		D		D			D		D		D		D	

		(%)		(%)		(%)		(%)		(%)		(%)		(%)		(%)
SiO_2	47.41	1%	46.17	0%	45.54	1%	40.60	1%	47.77	1%	48.82	1%	50.45	1%	47.82	1%
TiO_2	6.12	2%	5.62	2%	4.57	2%	2.15	2%	0.11	4%	0.25	2%	0.17	2%	0.08	4%
Al_2O_3	11.01	1%	11.66	0%	11.61	1%	13.42	1%	20.01	1%	17.11	1%	16.78	1%	19.25	2%
Fe_2O_3	17.70	1%	18.98	1%	21.32	1%	11.48	1%	2.80	1%	3.99	1%	3.29	1%	3.09	2%
MnO	0.25	1%	0.28	1%	0.35	1%	0.23	1%	0.05	1%	0.07	1%	0.06	3%	0.04	3%
MgO	5.12	1%	4.75	1%	3.58	0%	4.77	1%	9.54	2%	10.24	1%	11.57	1%	10.34	2%
CaO	8.76	2%	9.14	2%	8.24	1%	25.51	2%	12.57	2%	15.00	2%	11.56	2%	11.10	2%
Na_2O	3.47	1%	3.33	1%	4.28	2%	0.04	3%	2.66	1%	1.86	2%	2.94	2%	4.97	3%
K_2O	0.05	11%	0.03	8%	0.03	3%	0.02	7%	0.09	1%	0.04	1%	0.15	1%	0.03	5%
P_2O_5	0.11	1%	0.04	2%	0.49	4%	0.04	2%	0.02	4%	0.02	6%	0.01	6%	0.01	5%
LOI	*< 0.01*		*< 0.01*		*< 0.01*		1.75		4.39		2.61		3.01		3.28	
Total	100.00		100.00		100.00		100.00		100.00		100.00		100.00		100.00	

Li	6.64	2%	5.56	2%	17.4	1%	11.2	3%	28.7	2%	5.08	3%	14.5	3%	136	3%
Sc	513	2%	522	2%	466	1%	281	3%	164	2%	361	1%	266	3%	105	2%
Cr	1.50	14%	2.32	23%	2.12	62%	200	16%	1841	1%	1704	2%	2149	3%	549	1%
Co	45.2	1%	40.2	1%	43.3	2%	36.8	1%	30.1	1%	33.8	1%	31.5	1%	36.4	3%
Ni	6.68	3%	4.91	4%	3.16	6%	36.7	1%	339	1%	269	1%	433	1%	557	2%
Cu	55.2	6%	44.5	7%	59.4	8%	48.2	5%	153	2%	431	1%	37.1	3%	143	11%
Zn	146	2%	133	2%	179	1%	838	3%	24.7	6%	17.4	8%	20.4	3%	207	7%
Ga	20.9	1%	19.8	2%	25.8	1%	12.9	2%	9.21	4%	9.64	2%	8.27	3%	7.63	2%
As	0.279	11%	0.180	4%	1.64	14%	0.256	26%	*<0.214*		*<0.160*		0.220	1%	*<0.190*	
Rb	1.111	3%	0.7004	9%	1.25	2%	0.6900	6%	1.73	3%	0.717	4%	1.79	3%	0.9005	7%
Sr	985	1%	222.8	1%	446	2%	7.99	1%	315	2%	173	2%	238	3%	735	1%
Y	42.7	1%	29.1	1%	77.7	1%	13.0	2%	2.66	5%	7.01	2%	4.31	1%	1.57	3%
Zr	137	5%	69.4	7%	147	5%	22.7	11%	3.45	25%	9.93	31%	5.44	6%	2.20	17%
Nb	3.73	1%	1.85	3%	4.02	2%	0.567	5%	0.035	9%	0.083	5%	0.058	7%	0.012	21%
Sb	0.0	11%	0.0	24%	0.1	8%	0.1	81%	0.0	17%	0.1	8%	0.0	12%	0.0	53%

Cs	810.100	9%	400.052	8%	330.189	6%	680.576	2%	45 1.20	2%	730.054	5%	340.310	5%	500.266	5%
Ba	4.35	5%	4.07	2%	3.89	16%	2.47	4%	246	2%	2.03	5%	10.92	2%	632.25	4%
La	4.81	3%	0.3210	3%	4.37	3%	0.864	5%	0.2710	3%	0.347	3%	0.298	4%	0.268	4%
Ce	16.1	4%	0.8117	5%	16.1	4%	2.77	5%	0.8370	3%	1.27	1%	1.03	4%	0.7866	11%
Pr	2.84	3%	0.1449	3%	3.19	4%	0.495	6%	0.1410	3%	0.258	4%	0.192	3%	0.1155	7%
Nd	150	3%	0.9220	5%	18.5	5%	2.82	1%	0.7770	6%	1.52	2%	1.06	6%	0.5556	3%
Sm	4.50	3%	0.8590	5%	7.17	4%	1.29	3%	0.2860	12%	0.6672	2%	0.414	8%	0.1778	8%
Eu	1.66	4%	0.764	4%	3.22	4%	1.14	2%	0.2880	5%	0.3880	4%	0.293	5%	0.2170	7%
Gd	5.72	2%	3.38	2%	11.2	3%	1.82	2%	0.3780	6%	0.9500	5%	0.596	5%	0.2280	8%
Tb	1.08	1%	0.744	2%	2.05	2%	0.323	3%	0.0700	6%	0.182	3%	0.108	5%	0.0420	7%
Dy	7.45	2%	5.18	1%	13.9	3%	2.22	2%	0.4866	4%	1.27	5%	0.741	3%	0.2669	5%
Ho	1.59	2%	1.11	1%	2.95	3%	0.475	3%	0.093	4%	0.264	2%	0.159	3%	0.060	5%

Er	4.66	3%	3.23	2%	8.39	3%	1.37	4%	0.273	6%	0.754	3%	0.465	7%	0.157	8%
Tm	0.660	3%	0.458	2%	1.16	3%	0.192	5%	0.041	5%	0.102	4%	0.064	9%	0.022	7%
Yb	4.38	2%	2.96	4%	7.35	2%	1.26	6%	0.243	9%	0.670	2%	0.410	11%	0.150	12%
Lu	0.616	2%	0.418	3%	1.05	3%	0.175	6%	0.034	6%	0.09	5%	0.058	9%	0.023	13%
Hf	3.55	3%	2.03	9%	4.29	7%	0.652	11%	0.099	17%	0.325	19%	0.168	11%	0.072	22%
Ta	0.272	4%	0.135	3%	0.272	4%	0.038	8%	0.003	22%	0.006	26%	0.004	21%	0.002	13%
Th	0.114	7%	0.048	6%	0.093	14%	0.031	12%	0.002	22%	0.006	20%	0.004	42%	0.001	45%
U	0.061	3%	0.034	6%	0.073	9%	0.028	7%	0.010	10%	0.013	17%	0.016	12%	0.010	20%

LOI: loss of ignition
All Fe as Fe_2O_3

Table 3. Whole rock δ11B, δ18O and 87Sr/86Sr isotopic compositions of the Voltri Unit eclogites

Area	**Lithology**	**Sample**	**B (ppm)**	**$\delta^{11}B$ (‰)**	**1σ**	**$\delta^{18}O$ (‰)**	**$^{87}Sr/^{86}Sr_{meas}$**	**1σ**	**$^{87}Sr/^{86}Sr_{age}$**
Vara	Fe-Ti metagabbro	ENV 1	5.2	-0.65	0.37	+6.4	0.703696	0.000004	0.70368
		ENV 10/2	3.4	-3.18	0.21	+5.4	0.703676	0.000004	0.70363
		FL4	5.7	+0.93	0.18	+5.6	0.704192	0.000004	0.70415
	Metarodingite	ENV 11B	5.5	+11.54	0.24	+3.7	0.704608	0.000012	0.70447
Erro-	Mg-Al metagabbro	MG5	7.6	+4.30	0.03	+4.3[b]	0.703117	0.000003	0.70311

Tob bio	F1	3.2	+5.49	0.20	+3.1[b]	0.703026	0.000004	0.70302
	MG4/7	2.3[a]	+7.33	0.20	+4.7[b]	0.703387	0.000004	0.70337
	E89-26	4.7[a]	+10.00[a]	0.50[a]	+5.3[b]	0.703470[a]		
		repeated	+8.85	0.13		0.703468	0.000004	0.70347

[a]: data from Scambelluri & Tonarini (2012)
[b]: data from Früh-Green et al. (2001)
Age correction assume coheval metamorphic peak conditions for the Vara and Erro-Tobbio eclogites (~40Ma, Starr et al., 2020)

Table 4. Calculation for the flux of subducted B in eclogitized Mg-Al and Fe-Ti gabbros

		Volume (%)	**Density (g/cm3)**	**B (ppm)**	**Flux (g/year x106)**	**Flux (mol/year x106)**	**Flux contribution (%)**
Mid Atlantic Ridge	Mg-Al gabbros	28	3.3	4.5	9.05	0.84	77
	Fe-Ti gabbros	7	3.5	4.9	2.64	0.24	23
Southwest Indian Ridge	Mg-Al gabbros	78	3.3	4.5	25.20	2.33	82
	Fe-Ti gabbros	15	3.5	4.9	5.66	0.52	18

Volume % for Mid Atlantic Ridge from Godard et al. (2009)
Volume % for Southwest Indian Ridge from Ferrando et al. (2020)
Boron content is the average of B data reported in Table 3
Denity for Mg-Al gabbros is estimated by thermodynamic modeling.
Denity for Fe-Ti gabbros is assumed to be 0.2 g/cm3 higher than that of Mg-Al gabbros

Declaration of interests

☒ The authors declare that they have no known competing financial interests or personal relationships that could have appeared to influence the work reported in this paper.

- Eclogites from Fe-Ti and Mg-Al gabbros show negative and positive $\delta^{11}B$, respectively
- Metarodingite has positive $\delta^{11}B$ signature
- First report of eclogites with positive $\delta^{11}B$ signatures worldwide
- Potential inheritance of oceanic signatures up to eclogite facies conditions
- Subduction processes revealed by $\delta^{11}B$ rather than $\delta^{18}O$ and $^{87}Sr/^{86}Sr$ systems

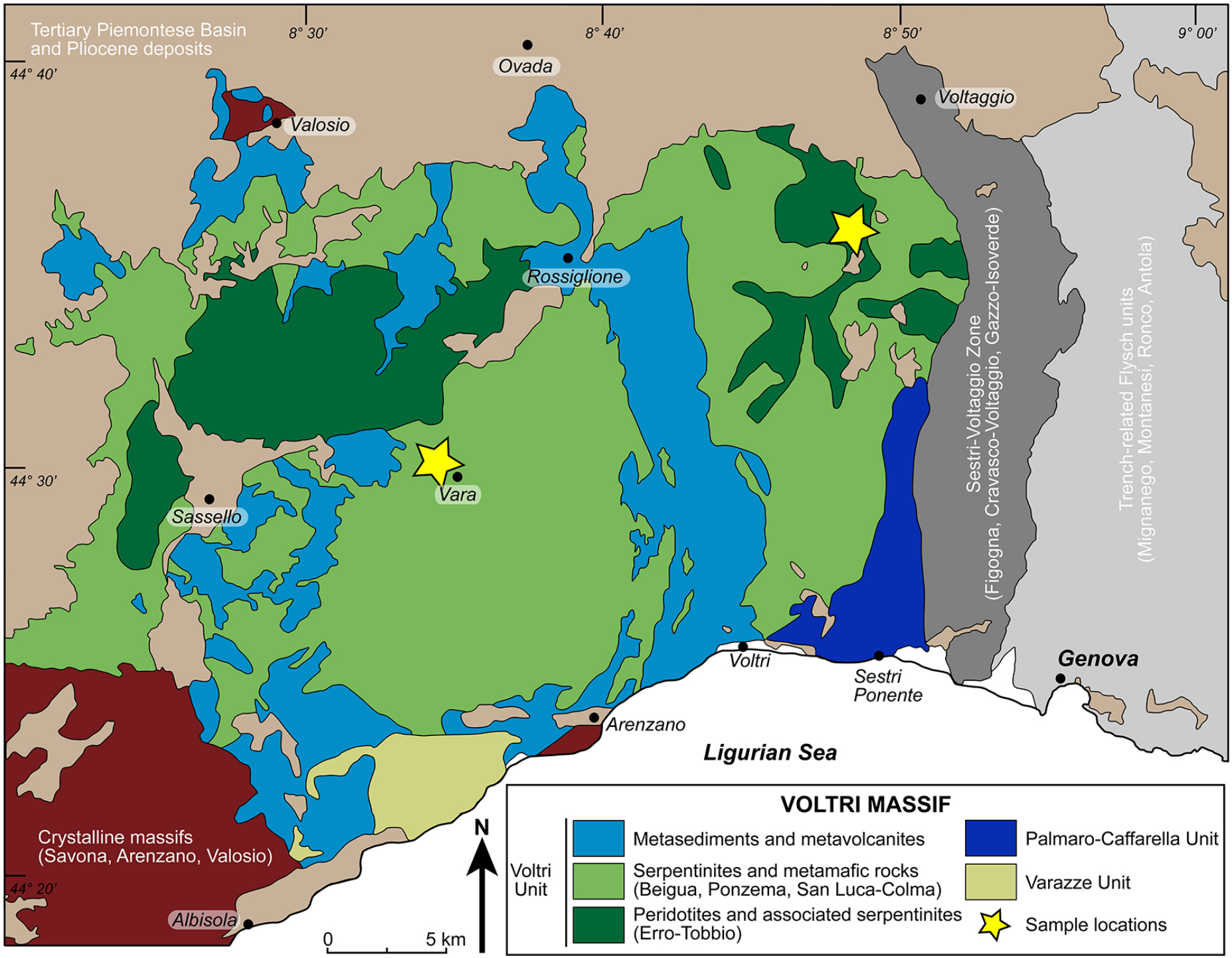
Tertiary Piemontese Basin
and Pliocene deposits
8° 30'
8° 40'
8° 50'
9° 00'
44° 40'
44° 30'
44° 20'
Ovada
Valosio
Voltaggio
Rossiglione
Vara
Sassello
Albisola
Arenzano
Voltri
Sestri
Ponente
Genova
Ligurian Sea
Sestri-Voltaggio Zone
(Figogna, Cravasco-Voltaggio, Gazzo-Isoverde)
Trench-related Flysch units
(Mignanego, Montanesi, Ronco, Antola)
Crystalline massifs
(Savona, Arenzano, Valosio)
N
0
5 km
VOLTRI MASSIF
Voltri
Unit
Metasediments and metavolcanites
Serpentinites and metamafic rocks
(Beigua, Ponzema, San Luca-Colma)
Peridotites and associated serpentinites
(Erro-Tobbio)
Palmaro-Caffarella Unit
Varazze Unit
Sample locations

Figure 1

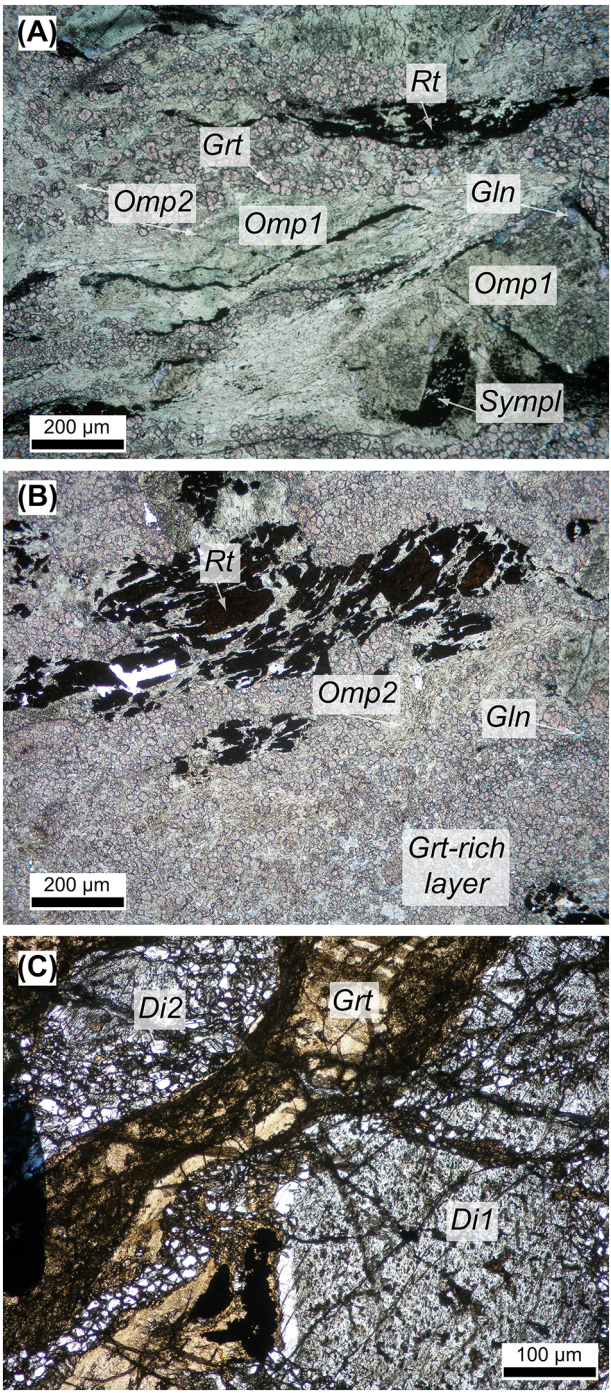
(A)
Rt
Grt
Omp2
Omp1
Gln
Omp1
Sympl
200 µm
(B)
Rt
Omp2
Gln
Grt-rich layer
200 µm
(C)
Di2
Grt
Di1
100 µm

Figure 2

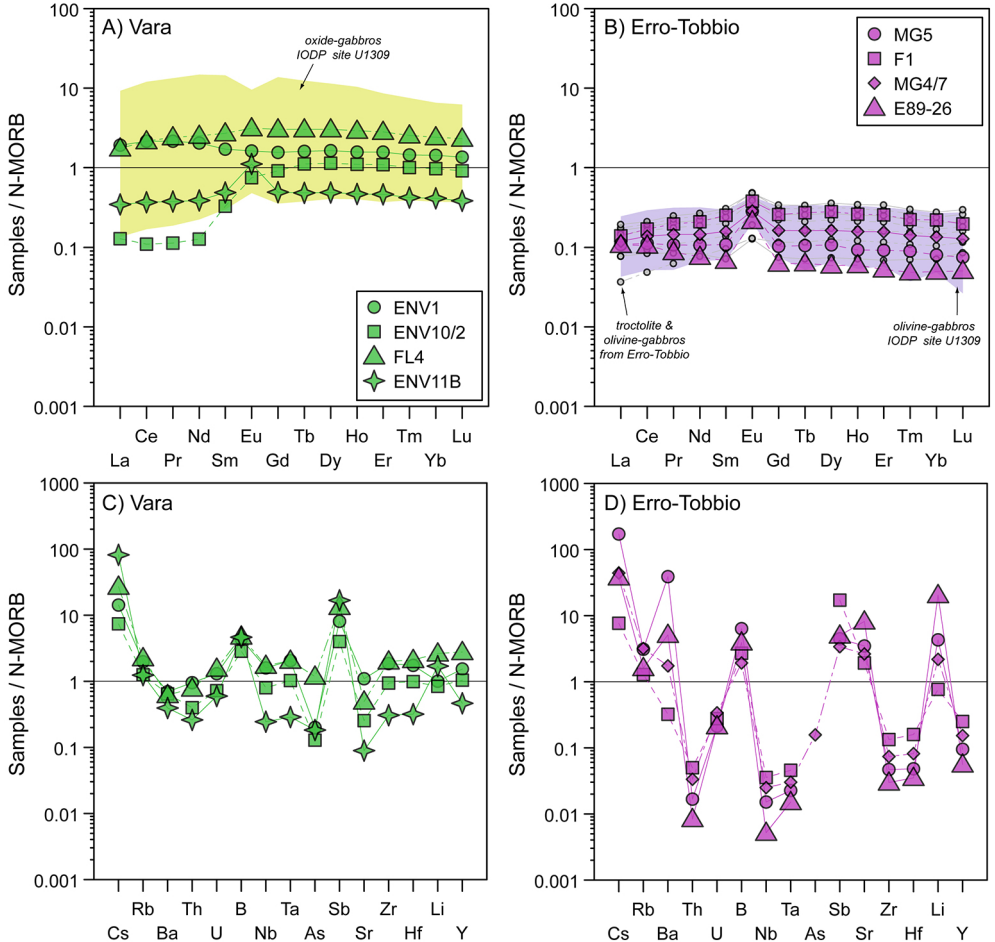
A) Vara
oxide-gabbros
IODP site U1309
ENV1
ENV10/2
FL4
ENV11B
B) Erro-Tobbio
MG5
F1
MG4/7
E89-26
troctolite &
olivine-gabbros
from Erro-Tobbio
olivine-gabbros
IODP site U1309
C) Vara
D) Erro-Tobbio
Samples / N-MORB
100
10
1
0.1
0.01
0.001
1000
La Ce Pr Nd Sm Eu Gd Tb Dy Ho Er Tm Yb Lu
Cs Rb Ba Th U B Nb Ta As Sb Sr Zr Hf Li Y

Figure 3

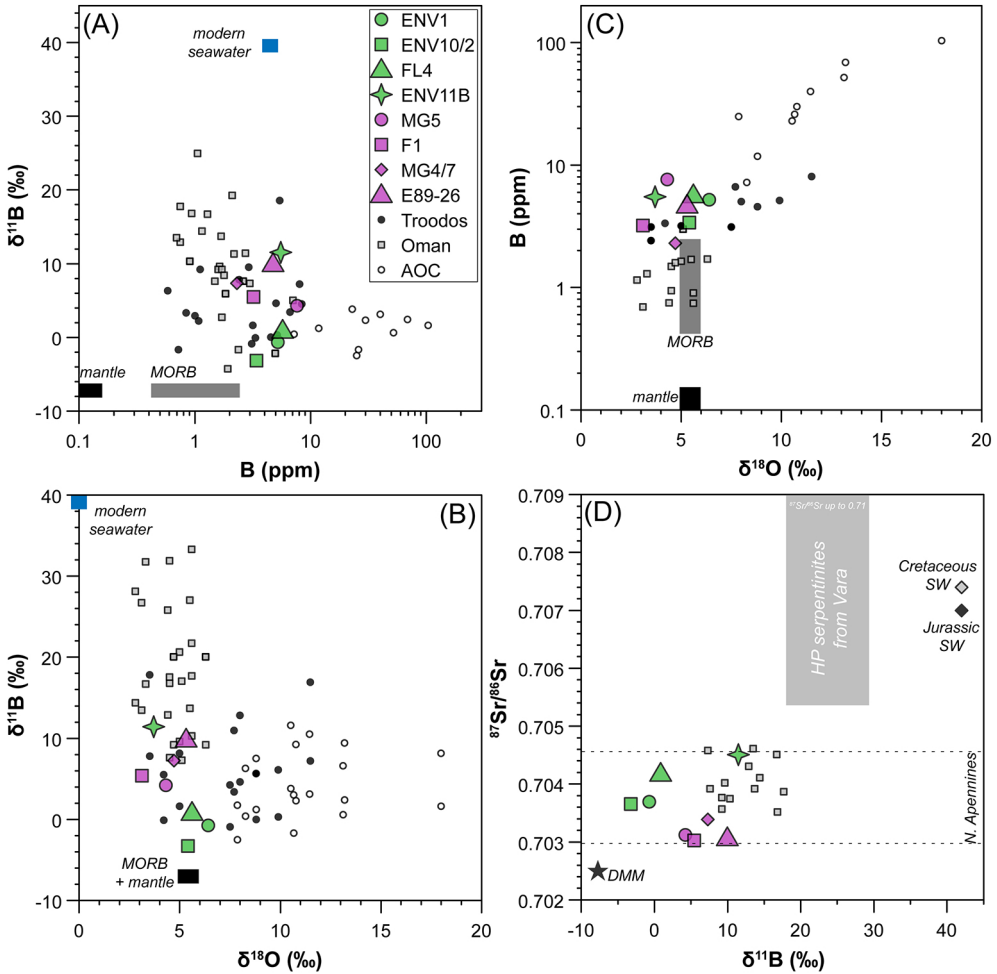
(A)
modern seawater
ENV1
ENV10/2
FL4
ENV11B
MG5
F1
MG4/7
E89-26
Troodos
Oman
AOC
mantle
MORB
δ11B (‰)
B (ppm)
(C)
B (ppm)
MORB
mantle
δ18O (‰)
(B)
modern seawater
MORB + mantle
δ11B (‰)
δ18O (‰)
(D)
87Sr/86Sr up to 0.71
HP serpentinites from Vara
Cretaceous SW
Jurassic SW
N. Apennines
DMM
87Sr/86Sr
δ11B (‰)

Figure 4

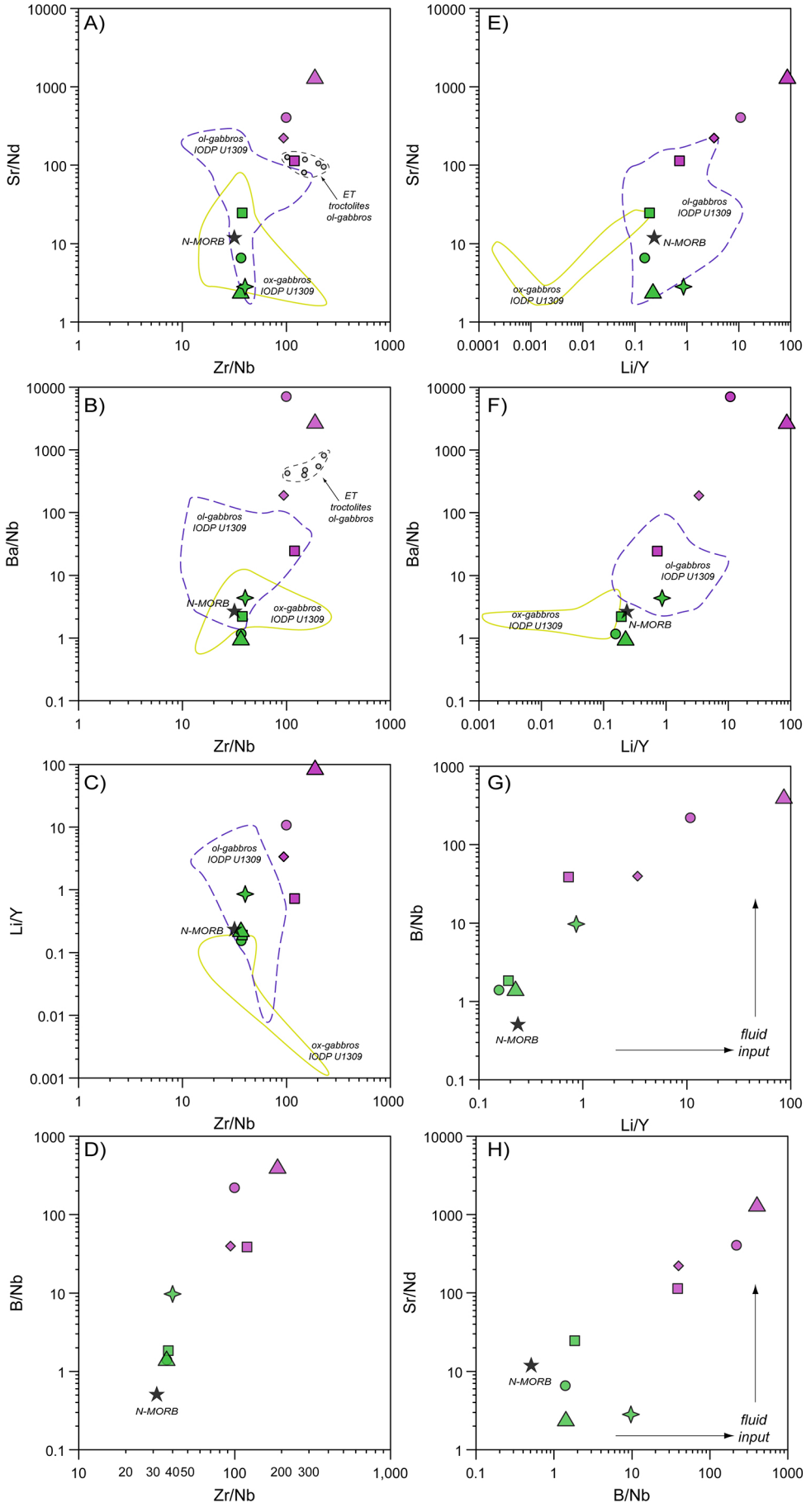
A)
Sr/Nd
Zr/Nb
ol-gabbros IODP U1309
ET troctolites ol-gabbros
N-MORB
ox-gabbros IODP U1309
E)
Sr/Nd
Li/Y
ol-gabbros IODP U1309
N-MORB
ox-gabbros IODP U1309
B)
Ba/Nb
Zr/Nb
ET troctolites ol-gabbros
ol-gabbros IODP U1309
N-MORB
ox-gabbros IODP U1309
F)
Ba/Nb
Li/Y
ol-gabbros IODP U1309
ox-gabbros IODP U1309
N-MORB
C)
Li/Y
Zr/Nb
ol-gabbros IODP U1309
N-MORB
ox-gabbros IODP U1309
G)
B/Nb
Li/Y
N-MORB
fluid input
D)
B/Nb
Zr/Nb
N-MORB
H)
Sr/Nd
B/Nb
N-MORB
fluid input

Figure 5

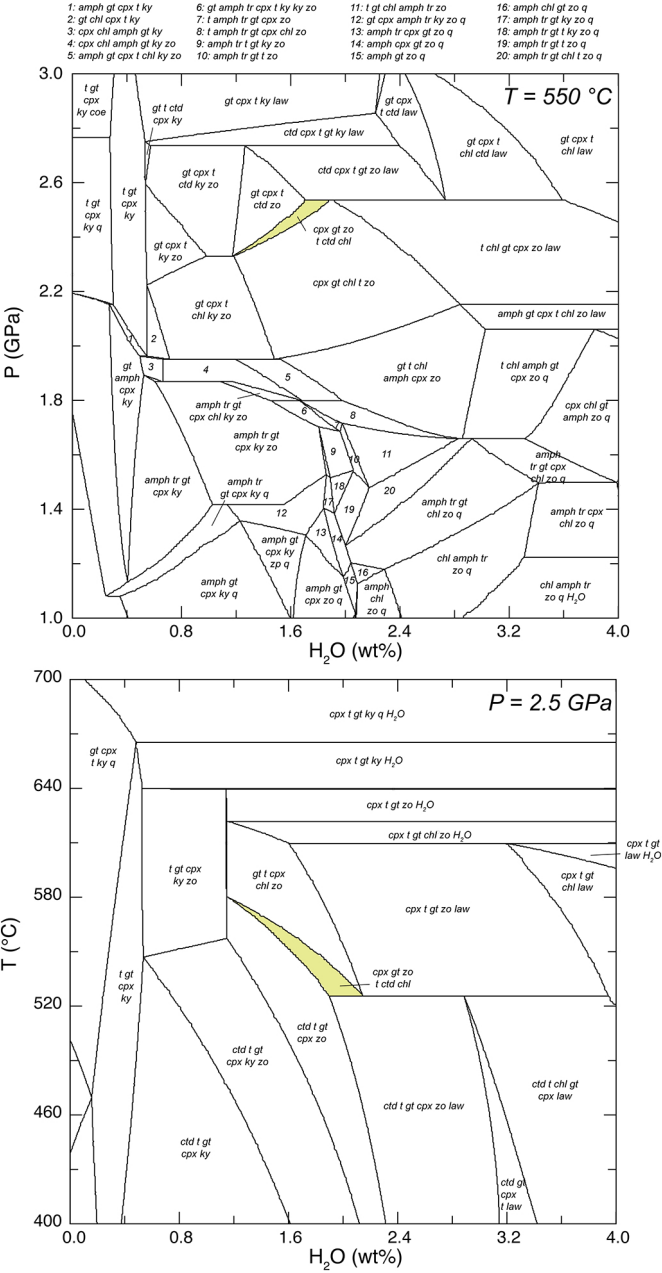
1: amph gt cpx t ky
2: gt chl cpx t ky
3: cpx chl amph gt ky
4: cpx chl amph gt ky zo
5: amph gt cpx t chl ky zo
6: gt amph tr cpx t ky ky zo
7: t amph tr gt cpx zo
8: t amph tr gt cpx chl zo
9: amph tr t gt ky zo
10: amph tr gt t zo
11: t gt chl amph tr zo
12: gt cpx amph tr ky zo q
13: amph tr cpx gt zo q
14: amph cpx gt zo q
15: amph gt zo q
16: amph chl gt zo q
17: amph tr gt ky zo q
18: amph tr gt t ky zo q
19: amph tr gt t zo q
20: amph tr gt chl t zo q
T = 550 °C
P (GPa)
H2O (wt%)
P = 2.5 GPa
T (°C)
H2O (wt%)

Figure 6

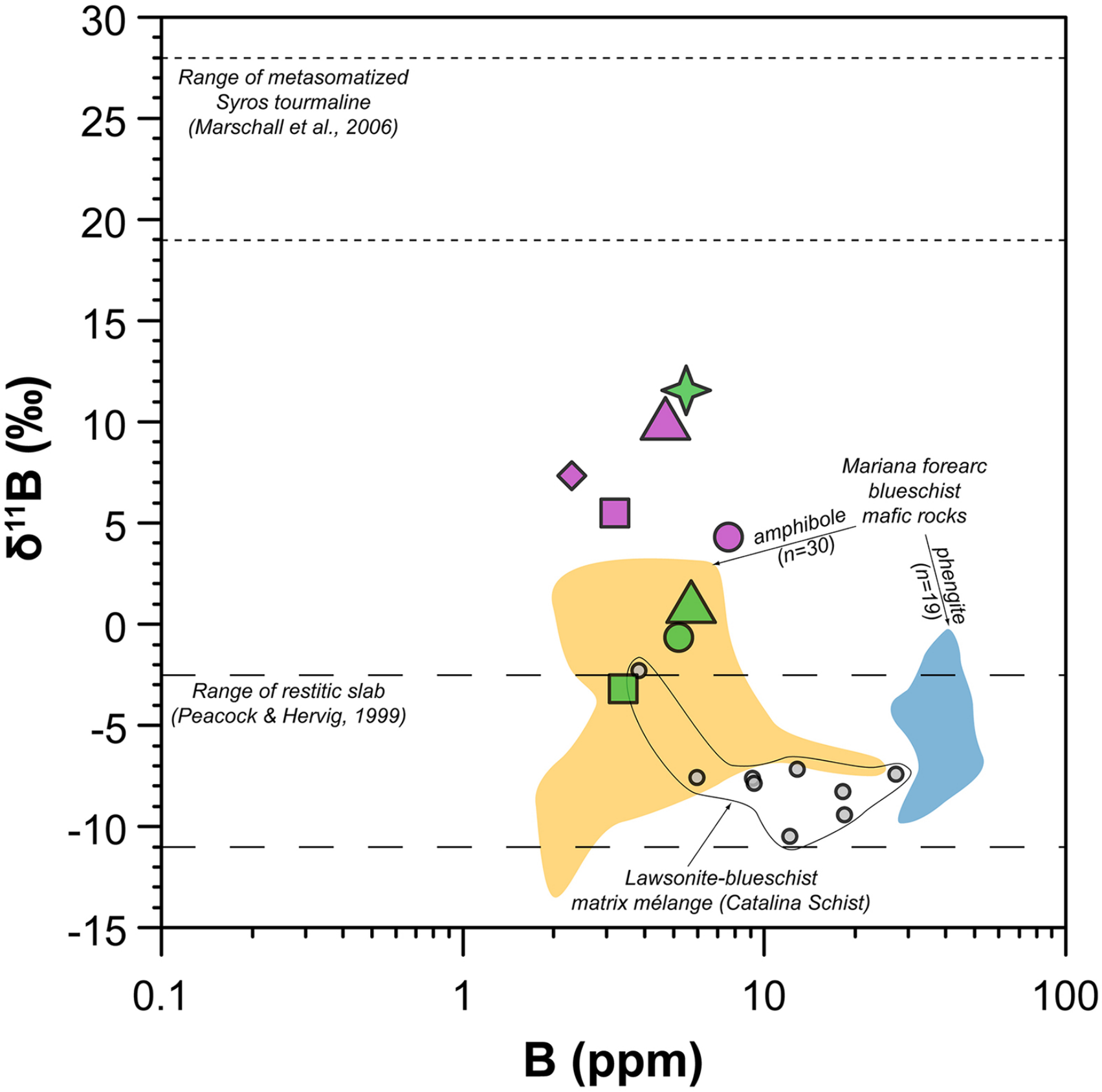
30
25
20
15
10
5
0
-5
-10
-15
δ11B (‰)
0.1
1
10
100
B (ppm)
Range of metasomatized
Syros tourmaline
(Marschall et al., 2006)
Range of restitic slab
(Peacock & Hervig, 1999)
Mariana forearc
blueschist
mafic rocks
amphibole
(n=30)
phengite
(n=19)
Lawsonite-blueschist
matrix mélange (Catalina Schist)

Figure 7

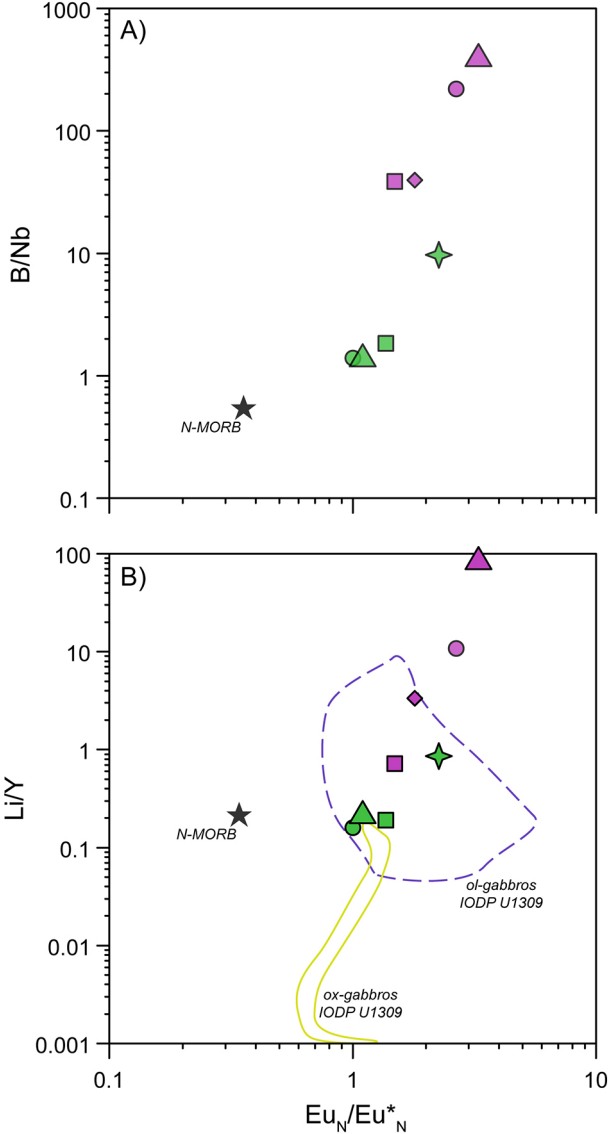
A)
B/Nb
1000
100
10
1
0.1
N-MORB
B)
Li/Y
100
10
1
0.1
0.01
0.001
N-MORB
ol-gabbros
IODP U1309
ox-gabbros
IODP U1309
0.1
1
10
Eu$_N$/Eu*$_N$

Figure 8

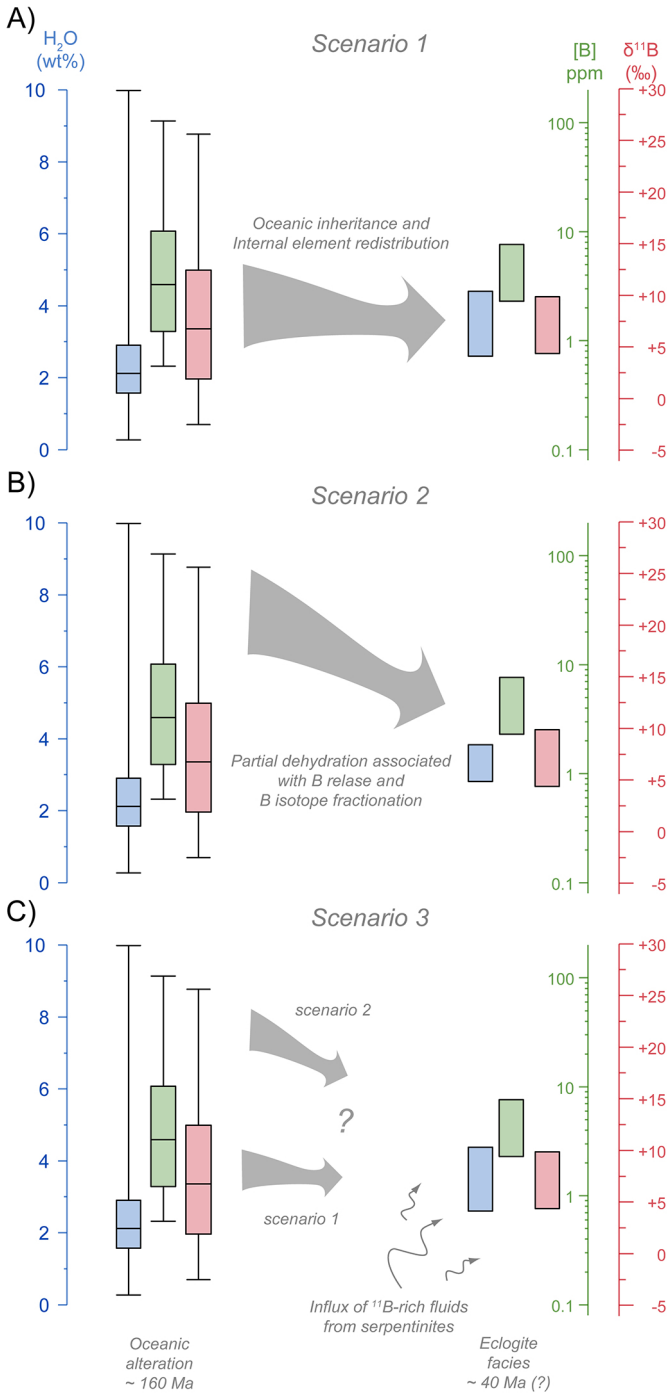
A)
H2O (wt%)
Scenario 1
[B] ppm
δ11B (‰)
Oceanic inheritance and Internal element redistribution
B)
Scenario 2
Partial dehydration associated with B relase and B isotope fractionation
C)
Scenario 3
scenario 2
?
scenario 1
Influx of 11B-rich fluids from serpentinites
Oceanic alteration ~ 160 Ma
Eclogite facies ~ 40 Ma (?)

Figure 9